Published in final edited form as:
Acta Biomater. 2011 June ; 7(6): 2355–2373. doi:10.1016/j.actbio.2011.03.016.

Bioactive glass in tissue engineering

Mohamed N. Rahaman[a,*], **Delbert E. Day**[a], **B. Sonny Bal**[b], **Qiang Fu**[c], **Steven B. Jung**[a,d], **Lynda F. Bonewald**[e], and **Antoni P. Tomsia**[c]

[a]Department of Materials Science and Engineering, and Center for Bone and Tissue Repair and Regeneration, Missouri University of Science and Technology, Rolla, MO 65409, USA

[b]Department of Orthopaedic Surgery, School of Medicine, University of Missouri, Columbia, MO 65211, USA

[c]Materials Sciences Division, Lawrence Berkeley National Laboratory, Berkeley, CA 94720, USA

[d]Mo-Sci Corporation, Rolla, MO 65409, USA

[e]Department of Oral Biology, School of Dentistry, University of Missouri–Kansas City, Kansas City, MO 64108, USA

Abstract

This review focuses on recent advances in the development and use of bioactive glass for tissue engineering applications. Despite its inherent brittleness, bioactive glass has several appealing characteristics as a scaffold material for bone tissue engineering. New bioactive glasses based on borate and borosilicate compositions have shown the ability to enhance new bone formation when compared to silicate bioactive glass. Borate-based bioactive glasses also have controllable degradation rates, so the degradation of the bioactive glass implant can be more closely matched to the rate of new bone formation. Bioactive glasses can be doped with trace quantities of elements such as Cu, Zn and Sr, which are known to be beneficial for healthy bone growth. In addition to the new bioactive glasses, recent advances in biomaterials processing have resulted in the creation of scaffold architectures with a range of mechanical properties suitable for the substitution of loaded as well as non-loaded bone. While bioactive glass has been extensively investigated for bone repair, there has been relatively little research on the application of bioactive glass to the repair of soft tissues. However, recent work has shown the ability of bioactive glass to promote angiogenesis, which is critical to numerous applications in tissue regeneration, such as neovascularization for bone regeneration and the healing of soft tissue wounds. Bioactive glass has also been shown to enhance neocartilage formation during in vitro culture of chondrocyte-seeded hydrogels, and to serve as a subchondral substrate for tissue-engineered osteochondral constructs. Methods used to manipulate the structure and performance of bioactive glass in these tissue engineering applications are analyzed.

Keywords

Bioactive glass; Tissue engineering; Scaffolds; Bone repair; Angiogenesis; Soft tissue repair; Chondrogenesis; Osteochondral tissues

*Corresponding author. Tel.: +1 573 341 4406. rahaman@mst.edu (M.N. Rahaman).

1. Introduction

Tissue engineering has emerged as a promising approach for the repair and regeneration of tissues and organs lost or damaged as a result of trauma, injury, disease or aging [1,2]. It has the potential to overcome the problem of a shortage of living tissues and organs available for transplantation. In the most common approach, a biomaterials scaffold with a well-defined architecture serves as a temporary structure for cells and guide their proliferation and differentiation into the desired tissue or organ. Growth factors and other biomolecules can be incorporated into the scaffold, along with the cells, to guide the regulation of cellular functions during tissue or organ regeneration [3–6]. The overall purpose of this scaffold-based tissue engineering approach is to provide the temporary support structure for tissue forming cells to synthesize new tissue of the desired shape and dimensions.

The last two decades have seen a dramatic growth in the field of tissue engineering. These efforts have resulted in cell-based regeneration of individual tissues such as skin [7–10], bone [11–13] and cartilage [14,15]. Recent work in cell-based restoration of multiple tissue phenotypes by composite tissue grafts, such as osteochondral and fibro-osseous grafts, have shown promising results for the tissue-engineered regeneration of complex anatomical structures such as the synovial joint condyle, bone–tendon complex, bone–ligament junction and the periodontium [16].

These advances would not have been possible without the innovative design and fabrication of biomaterials and scaffolds. Biomaterials used for creating scaffolds are designed to meet a set of stringent requirements that are either essential or desirable for optimized tissue formation [17]. Scaffolds, as mentioned earlier, must provide a temporary structure for cells to synthesize new tissue but must undergo degradation upon neogenesis of that tissue. The architecture of the scaffold is critical for providing cells with an optimized microenvironment to synthesize new tissue and to allow flow or diffusion of nutrients between the cells and the surrounding environment. Recent advances in innovative materials processing such as electrospinning, solid freeform fabrication (rapid prototyping) and unidirectional freezing of suspensions offer considerable promise for tissue regeneration using cell-based therapies [18–22].

The purpose of this article is to evaluate the role and impact of one particular subset of biomaterials in tissue engineering applications, namely: bioactive glass for hard and soft tissue regeneration. The focus is on recent developments of new bioactive glasses and their conversion into scaffolds with the requisite anatomical shape and architecture. Methods that can be used to manipulate the materials structure and the variables that affect the materials performance in these tissue engineering applications are analyzed.

2. Scaffolds for tissue engineering

The ideal scaffold should (i) be biocompatible (not toxic) and should promote cell adhesion and proliferation; (ii) exhibit, after in vitro tissue culture, mechanical properties that are comparable to those of the tissue to be replaced; (iii) have a porous three-dimensional (3-D) architecture to allow cell proliferation, vascularization and diffusion of nutrients between the cells seeded within the matrix and the surroundings; (iv) degrade at a rate that matches the production of new tissue, into nontoxic products that can be easily resorbed or excreted by the body; and (v) be capable of being processed economically into anatomically relevant shapes and dimensions, and be sterilized for clinical use.

Scaffolds for tissue engineering are commonly constructed from biodegradable polymeric materials, synthetic or natural [23–28]. However, for the regeneration of load-bearing bones, the use of biodegradable polymer scaffolds is challenging because of their low mechanical

strength. Attempts have been made to reinforce the biodegradable polymers with a biocompatible inorganic phase, commonly hydroxyapatite (HA) [29–32]. Although brittle, scaffolds fabricated from inorganic materials such as calcium phosphate-based bioceramics and bioactive glass can provide higher mechanical strength than polymeric scaffolds. Biodegradable metals are currently under investigation [33], but their corrosion behavior in vivo remains a key concern.

Calcium phosphate-based bioceramics, such as HA, $Ca_{10}(PO_4)_6$-$(OH)_2$, β-tricalcium phosphate (β-TCP), $Ca_3(PO_4)_2$, and biphasic calcium phosphate (BCP), a mixture of HA and β-TCP that is composed of the same ions as bone, are the inorganic materials which have received most attention for bone repair applications [34–37]. When compared to β-TCP, HA resorbs slowly and undergoes little conversion to a bone-like material after implantation [38,39]. However, for the same porosity, β-TCP scaffolds often have lower strength than HA scaffolds, so their use in the repair of load-bearing bones may be challenging. The use of BCP with different HA to β-TCP ratios allows manipulation of the degradation rate [40], as well as other properties [41].

Bioactive glass and glass–ceramics are also used in bone repair applications and are being developed for tissue engineering applications [42–45]. Bioactive glass has an amorphous structure, whereas glass–ceramics are crystallized glasses, consisting of a composite of a crystalline phase and a residual glassy phase. There has been heightened interest in the science and biomedical application of bioactive glass over the last two decades, as evidenced by the growing number of publications in the field (Fig. 1).

3. Bioactive glass

In a general sense, a bioactive material has been defined as a material that has been designed to induce specific biological activity [46]. In a more narrow sense, a bioactive material has been defined as a material that undergoes specific surface reactions, when implanted into the body, leading to the formation of an HA-like layer that is responsible for the formation of a firm bond with hard and soft tissues [47]. The ability of a material to form an HA-like surface layer when immersed in a simulated body fluid (SBF) in vitro is often taken as an indication of its bioactivity [48]. Furthermore, it has been suggested that this in vitro bioactivity is an indication of the bioactive potential of a material in vivo [49]. However, this narrow definition of bioactivity has been called into question recently [50]. Dicalcium phosphate dihydrate, for example, shows the formation of an HA-like surface layer when immersed in a SBF in vitro, but no direct bone bonding in vivo [51–53]. Furthermore, β-TCP does not always lead to the formation of an HA-like material in an SBF despite its extensive bonding to bone [54].

3.1. Silicate bioactive glass

Since the report of its bone-bonding properties nearly 40 years ago [55], the bioactive glass designated 45S5, sometimes referred to by its commercial name Bioglass®, has been the most widely researched glass for biomedical applications [44]. This glass is a silicate glass based on the three-dimensional (3-D) glass-forming SiO_2 network in which Si is fourfold coordinated to O. The key compositional features that are responsible for the bioactivity of 45S5 glass are its low SiO_2 content (when compared to more chemically durable silicate glasses), high Na_2O and CaO (glass network modifiers) content, and high CaO/P_2O_5 ratio (Table 1).

The mechanisms of bioactivity and bone bonding of 45S5 glass have been widely studied, and described in detail elsewhere [44,56,57]. Based on those studies, the bonding of 45S5 glass to bone has been attributed to the formation of a carbonate-substituted hydroxyapatite-

like (HCA) layer on the glass surface in contact with the body fluid. Because this HCA layer is similar to the mineral constituent of bone, it bonds firmly with living bone and tissue. While some details of the chemical and structural changes are not clear, the HCA layer is generally believed to form as a result of a sequence of reactions on the surface of the bioactive glass implant, as described by Hench [44]:

Stage 1: Rapid ion exchange reactions between the glass network modifiers (Na^+ and Ca^{2+}) with H^+ (or H_3O^+) ions from the solution, leads to hydrolysis of the silica groups and the creation of silanol (Si−OH) groups on the glass surface: e.g.

$$\mathrm{Si-O-Na^+ + H^+ \rightarrow Si-OH + Na^+(aq)} \quad (1)$$

The pH of the solution increases due to the consumption of H^+ ions.

Stage 2: The increase in pH (or OH^- concentration) leads to attack of the SiO_2 glass network, and the dissolution of silica, in the form of silicic acid, $Si(OH)_4$, into the solution, and the continued formation of Si−OH groups on the glass surface:

$$\mathrm{Si-O-Si + H_2O \rightarrow Si-\mathit{OH} + OH-Si} \quad (2)$$

While the solubility of silica is low, the products of 45S5 glass and glass–ceramic dissolution in aqueous solutions have shown an increase in Si concentration [58], indicating that dissolution of silica is an important mechanism. However, other mechanisms could also contribute to the increase in Si concentration.

Stage 3: Condensation and polymerization of an amorphous SiO_2-rich layer (typically 1–2 μm thick) on the surface of the glass depleted in Na^+ and Ca^{2+}.

Stage 4: Further dissolution of the glass, coupled with migration of Ca^{2+} and $(PO_4)^{3-}$ ions from the glass through the SiO_2-rich layer and from the solution, leading to the formation of an amorphous calcium phosphate (ACP) layer on the surface of the SiO_2-rich layer.

Stage 5: The glass continues to dissolve, as the ACP layer incorporates $(OH)^-$ and $(CO_3)^{2-}$ from the solution and crystallizes as an HCA layer.

With the initial formation of an HCA layer, the biological mechanisms of bonding to bone are believed to involve adsorption of growth factors, followed by attachment, proliferation and differentiation of osteoprogenitor cells [59]. Osteoblasts (bone-forming cells) create extracellular matrix (collagen), which mineralizes to form a nanocrystalline mineral and collagen on the surface of the glass implant while the degradation and conversion of the glass continues over time [60].

The biocompatibility of 45S5 glass has long been established [61]. As described above, upon implantation, 45S5 bioactive glass undergoes chemical degradation, releasing ions such as Na^+ and Ca^{2+}, and conversion to an HCA material. Silicon, presumably in the form of silicic acid, $Si(OH)_4$, is also released during the degradation by dissolution or by other mechanisms, such as small pieces of silica-rich material eaten by phagocytes and excreted out. The release of Si from 45S5 granules implanted in the muscle and tibiae of rabbits has been studied to determine the pathway of silicon released during the degradation of the glass in vivo [62]. By measuring the silicon released in urine and blood samples for up to 7 months post-implantation, and using chemical and histopathological analyses of bone tissue

and several organs, it was found the silicon resulting from the 45S5 degradation was harmlessly excreted in soluble form through the urine.

45S5 glass remains the gold standard for bioactive glass but, as a scaffold material, it has several limitations. One limitation is the difficulty of processing 45S5 glass into porous 3-D scaffolds. Porous bioactive glass scaffolds are commonly prepared by heating (sintering) glass particles, already formed into the desired 3-D geometry, to bond the particles into a strong glass phase containing an interpenetrating network of pores. Because of the limited ability of 45S5 glass to sinter by viscous flow above its glass transition temperature (T_g), and the narrow window between T_g and the onset of crystallization, severe difficulties are encountered in sintering the particles into a dense network. Consequently the scaffold often has low strength [63]. Commonly, the glass devitrifies during sintering to form a predominantly combeite crystalline phase ($Na_2O{-}2CaO{-}3SiO_2$). While devitrification does not inhibit the ability of 45S5 glass to form an HA-like surface layer, it has the effect of reducing the rate of conversion to HA [64]. Another limitation of 45S5 glass is its slow degradation rate and conversion to an HA-like material [56,57], which makes it difficult to match the degradation rate of the scaffold with the rate of new tissue formation. The conversion of the scaffold to an HA-like material is often incomplete, so therefore a portion of unconverted glass containing SiO_2 could remain in the scaffold, raising uncertainty about the long-term effects of SiO_2 in vivo.

A complication with the use of 45S5 glass and other bioactive glasses and other biodegradable materials is that the local biological microenvironment can be influenced significantly by their degradation. Increases in the concentration of ions, such as Na^+ and Ca^{2+}, and changes in the pH occur as a result of the degradation, particularly in the early stages when the degradation rate is fast [56,57,65,66]. The biological effects of these changes are difficult to predict from in vitro experiments. Furthermore, the biological roles of these soluble species, their toxicity and their removal are often not clearly understood.

A silicate bioactive glass designated 13–93 [67,68] is based on the 45S5 composition, but it has a comparatively higher SiO_2 content and additional network modifiers, such as K_2O and MgO, when compared to 45S5 (Table 1). Products of 13–93 glass have been approved for in vivo use in Europe. Because 13–93 has better processing characteristics by viscous flow sintering (larger window between T_g and the onset of crystallization), the glass phase in porous 3-D scaffolds can be sintered to high density without crystallization. In vitro cell culture showed no marked difference in the proliferation and differentiated function of osteoblastic MC3T3-E1 or MLO-A5 between dense disks of 45S5 and 13–93 glass [69]. However, 13–93 glass degrades (and converts to an HA-like material) more slowly than 45S5 glass.

3.2. Borate bioactive glass

More recent work has shown that certain compositions in other glass-forming systems, such as borate glass [70–74], are also bioactive (Table 1). Because of their lower chemical durability, some borate bioactive glasses degrade faster and convert more completely to an HA-like material, when compared to silicate 45S5 or 13–93 glass [56,57,65,66]. The conversion of borate bioactive glass to HA appears to follow a process similar to that described for 45S5 glass, but without the formation of a SiO_2-rich layer [56,57].

Borate bioactive glasses have been shown to support cell proliferation and differentiation in vitro [75,76], as well as tissue infiltration in vivo [77]. Borate bioactive glasses have also been shown to serve as a substrate for drug release in the treatment of bone infection [78–80]. A concern associated with borate bioactive glass is the toxicity of boron released into the solution as borate ions, $(BO_3)^{3-}$. In conventional “static” in vitro culture conditions,

some borate glasses were observed to be toxic to cells, but the toxicity was diminished in "dynamic" culture conditions [81]. Scaffolds of a borate bioactive glass, designated 13–93B3, with a composition obtained by replacing all the SiO_2 in 13–93 glass with B_2O_3 (Table 1), were found to be toxic to murine MLO-A5 osteogeneic cells in vitro [77]. However, the same scaffolds did not show toxicity to cells in vivo and supported new tissue infiltration when implanted subcutaneously in rats [77,82]. Borate glass pellets implanted in rabbit tibiae produced boron concentrations in the blood far below the toxic level [80].

Recent work has shown the ability to control the degradation rate of bioactive glass by manipulating its composition. For example, by partially replacing the SiO_2 in silicate 45S5 or 13–93 glass with B_2O_3 (yielding a borosilicate bioactive glass), or fully replacing the SiO_2 with B_2O_3 (producing a borate bioactive glass), the degradation rate can be varied over a wide range [56,57,65]. The ease of manufacture and the ability to control the degradation rate of these borate-based glasses make them particularly useful for promoting the regeneration of bone. By controlling the glass composition, it should be possible to match the degradation rate of borate-based bioactive glass with the bone regeneration rate. Another possibility is to exploit the compositional flexibility of glass so that it also can serve as a source of many of the minor elements known to favor bone growth, such as Zn, Cu, F, Mn, Sr and B. As the glass degrades in vivo, these elements are released at a biologically acceptable rate.

3.3. Phosphate bioactive glass

Phosphate glasses, based on the P_2O_5 glass-forming network and CaO and Na_2O as modifiers (Table 1), have also been developed for biomedical use [83–87]. As their constituent ions are present in the organic mineral phase of bone, these glasses have a chemical affinity with bone. The solubility of these glasses can be controlled by modifying their composition; therefore these glasses may have additional clinical potential as resorbable materials.

4. Osteoconductivity and osteoinductivity of bioactive glass

Bioactive glass (45S5) has been shown to enhance new bone formation in vivo [88,89]. When implanted in the rabbit femurs, granules of 45S5 bioactive glass were found to promote more rapid bone proliferation than (synthetic) HA [90]. HA is classified as osteoconductive, because it supports new bone growth along the implant at the bone–implant interface. However, 45S5 glass is considered to be osteoconductive as well as osteoinductive, because it supports new bone growth along the bone–implant interface as well as within the implant away from the bone–implant interface.

Since the stimulation of osteoinduction provides a desirable benefit for bone regeneration, studies have been performed to understand the mechanism by which 45S5 glass induces this response. The signals that 45S5 glass provides to cells in order to guide them to create new bone have been investigated [91–93]. As described earlier, as 45S5 glass degrades it releases Na^+ and Ca^{2+} ions, and soluble silica, presumably in the form of $Si(OH)_4$. It is believed that a combination of some of these ions triggers cells to produce new bone [59]. In particular, the concentrations of Ca^{2+} and $Si(OH)_4$ are thought to be critical. However, the role of Si has been called into question. A recent review showed no evidence of Si release from Si-substituted calcium phosphates, and found no study linking the improved biological performance of Si-substituted calcium phosphates to Si release [94]. Furthermore, recent work has shown that certain compositions of borate bioactive glass enhance new bone formation to a greater extent than 45S5 glass, although these borate glasses contain no Si [95].

5. Bioactive glass scaffolds for bone regeneration

The most common method for preparing porous bioactive glass scaffolds is to form glass particles (or short fibers) of a "melt-derived" glass (produced using conventional glass processing techniques) into a construct with the desired architecture and geometry; this construct is subsequently sintered to bond the particles (or fibers) into a mechanically reliable 3-D network with interconnected porosity. A method that is used far less frequently is sol–gel processing of a solution. More recently, electrospinning of a solution or processing of a viscous melt has been used to prepare pliable scaffolds of bioactive glass consisting of nanofibers.

5.1. Melt-derived bioactive glass scaffolds

As summarized in Table 2, a variety of methods can be used to form the particles of a melt-derived bioactive glass into a porous construct, producing different pore architectures (Fig. 2). For a given bioactive glass scaffold, the porosity, pore size and pore inter-connectivity are critical parameters. In general, interconnected pores with a mean diameter (or width) between neighboring pores of 100 μm or greater, and open porosity of >50% are generally considered to be the minimum requirements to permit tissue ingrowth and function in porous scaffolds [96,97].

As described earlier, one of the simplest methods for forming a scaffold is to thermally bond a loose, random packing of particles or short fibers in a mold with the desired geometry [98–101] (Fig. 2a and b). Common limitations include a fairly narrow porosity range (40–50%), and the potential for constricted connectivity between neighboring pores. Another method is to mix the bioactive glass particles with a fugitive phase (e.g. NaCl, or an organic material such as starch) that is removed by dissolution or decomposition after forming but prior to sintering. However, constricted connectivity between neighboring pores still remains a problem here as well.

The polymer foam replication technique can provide a scaffold microstructure that is similar to that of dry human trabecular bone (Fig. 2c). Scaffolds of silicate, borosilicate and borate bioactive glass have been prepared with porosities in the range 60–90% using this method [63,66,76,102,103]. In the case of 45S5 glass, the aforementioned crystallization leads to glass–ceramic scaffolds with low strength (<1 MPa) (Table 2). However, silicate 13–93 glass and borate 13–93B3 bioactive glass scaffolds have higher compressive strength and elastic modulus values, in the range reported for trabecular bone (strength, 2–12 MPa; elastic modulus, 0.1–5 GPa).

Freezing of aqueous solutions and suspensions has been used to prepare polymeric and ceramic materials with disordered macro-porous structures [104,105]. By carrying out the freezing process in a controlled manner so that the ice grows in a preferred direction, porous scaffolds with an oriented microstructure have been prepared [22,106–109]. A benefit of the oriented microstructure is the higher scaffold strength in the direction of orientation, compared to the strength of a scaffold with a randomly oriented micro-structure [22]. Porous bioceramic scaffolds prepared from aqueous suspensions often have a lamellar microstructure in which the small pore widths (10–40 μm) are unfavorable for supporting tissue ingrowth. By modifying the composition of the aqueous solvent in the suspensions, through the use of water–dioxane mixtures [108–110], or an organic phase (camphene) as the sub-limable vehicle [111], bioactive glass (13–93) scaffolds with columnar microstructures and pore diameters of 100–150 μm have been prepared (Fig. 2d and e). In addition to their higher strength, these oriented bioactive glass scaffolds have shown the ability to support cell proliferation and differentiation in vitro, as well as tissue infiltration in vivo [110,112].

Solid freeform fabrication (SFF) or rapid prototyping methods provide the ability to produce scaffolds with customized external shape and predefined internal microarchitecture. This can be used to control the porosity, pore size and pore size distribution, as well asto create structures to improve tissue ingrowth and diffusion of nutrients into the scaffold. SFF methods involve building 3-D objects layer by layer from a computer-generated model using computer-aided design (CAD) software [113]. Data obtained from computerized tomography or magnetic resonance imaging scans can be used to create a customized CAD model, and consequently a scaffold possessing the precise external dimensions required to correct the damaged tissue site.

SFF has seen significant use in the fabrication of scaffolds from biodegradable polymers (e.g. poly(lactic-co-glycolic acid) (PLGA), poly(caprolactone) (PCL)), and the method has also been used to prepare scaffolds of calcium phosphate materials (e.g. HA, TCP), as well as composites of these two classes of materials (e.g. PLGA/TCP) [114–116]. The fabrication of composite scaffolds containing bioactive glass (e.g. PLA/45S5 glass; PCL/45S5 glass) using a robocasting SFF technique has been reported [117]. Recently, the production of silicate bioactive glass scaffolds using SFF methods, such as robocasting [118], freeze extrusion fabrication [119] and selected laser sintering [120], has been reported. In the robocasting method, the scaffold is formed by printing a concentrated suspension (an ink) through a narrow-diameter nozzle onto a substrate using a robotic deposition device. After drying, the as-formed construct is heated slowly (to 700 °C for 6P53B glass) to decompose the organic phase and thermally bond the particles. Fig. 2f shows an example of a 6P53B bioactive glass scaffold formed by the robocasting method. As shown, this scaffold has a porosity of 60%, struts with a diameter of 500 μm, and pores of width 500 μm, but both the porosity and pore width can be controlled by altering the thickness and spacing of the extruded filaments. A notable feature of the scaffold is the dense 3-D network of the bioactive glass and the uniform microstructure which, as described later, result in a high compressive strength, comparable to that of cortical bone.

5.2. Sol–gel-derived bioactive glass scaffolds

A sol–gel process, involving the foaming of a sol with the aid of a surfactant, followed by condensation and gelation reactions, has been used to prepare porous scaffolds of a few bioactive glasses, such as the glass designated 58S, with the composition (mol.%): 60 SiO_2, 36 CaO, 4 P_2O_5 [121]. The as-prepared scaffold has an overall microstructure similar to that of dry human trabecular bone, but the pore structure is hierarchical, consisting of interconnected macropores (>100 μm) resulting from the foaming process and nanopores (less than several tens of nanometers) that are inherent to the sol–gel process [122]. This hierarchical pore structure of the scaffold is beneficial for stimulating interaction with cells as it mimics the hierarchical structure of natural tissues and more closely simulates a physiological environment. Because of the nanopores in the glass, sol–gel-derived scaffolds have high surface area (100–200 $m^2\ g^{-1}$). As a result, these scaffolds degrade and convert faster to HA than scaffolds of melt-derived glass with the same composition. However, these sol–gel-derived scaffolds have low strength (2–3 MPa) [123], and consequently they are suitable for substituting defects in low-load sites only.

5.3. Nanofibrous bioactive glass scaffolds

A recent development in scaffold-based tissue engineering is the use of an electrospinning technique to create nanofibrous scaffolds of biodegradable polymers which mimic the fibrous structure of the extracellular matrix [19,20]. The technique is also being applied to the formation of fibers with submicron or nanoscale diameters, and to nanofibrous scaffolds of bioactive glass [124,125]. Because of their high surface area, bioactive glass nanofibers degrade rapidly and convert to HA. As in the case of sol–gel-derived bioactive glasses, the

bioactivity of these glass nanofibers is maintained over a larger SiO_2 compositional range when compared to melt-derived glasses.

Nanofibrous scaffolds of bioactive glass have been prepared by electrospinning organic/inorganic solutions (Fig. 3a). A mixture of tetraethyl orthosilicate and calcium nitrate, for example, is typically used as the starting solution for the preparation of 70S30C glass (70 mol.% SiO_2, 30 mol.% CaO) by the sol–gel process described above [124,125]. After the electrospinning step, the as-prepared nanofibrous scaffolds are heated to 600–700 °C to decompose residual organic or inorganic groups (e.g. ethyl, nitrate). Bioactive glass fibers with diameters in the micron to sub-micron range, prepared from a melt-derived glass, are available commercially (Fig. 3b). This material, which is very pliable and has a rapid degradation rate because of its fine fiber diameter, has potential applications in the regeneration of non-loaded bone defects and the healing of soft tissue.

6. In vitro characteristics of bioactive glass scaffolds

The in vitro characteristics of bioactive glass scaffolds, such as the degradation rate and conversion to an HA-like material, mechanical response and response to cells, are dependent primarily on the glass composition and the microstructure (architecture) of the scaffolds.

6.1. Degradation and conversion to hydroxyapatite

As previously described, the mechanisms by which silicate, borosilicate and borate bioactive glass degrade and convert to an HA-like material have been the subject of several investigations. While the general mechanistic features are believed to be understood [44,56,57], the influence of the glass composition on the structure of the HA-like conversion product remains unclear.

Typically, the kinetics of degradation of the glass and conversion to HA in vitro have been evaluated by immersing the glass (in the shape of particles, a disc or a porous scaffold) in an aqueous phosphate solution such as SBF at 37 °C, and measuring the weight loss of the glass as a function of time [56,57,65,66] (Fig. 4a). In addition, the conversion product has been characterized using structural, chemical and microchemical techniques. The degradation is accompanied by the dissolution of ions and soluble species (e.g. Na^+, $(BO_3)^{3-}$ and $Si(OH)_4$, depending on the glass composition) into the solution, so there is also a change in the pH (Fig. 4b) and the ionic concentration of the solution as a function of time.

Analysis of the kinetics indicates that the mechanism of conversion to HA depends on the bioactive glass composition [66,126]. The reaction is pseudomorphic (the external dimensions of the product are nearly identical to that of the starting material), starting at the surface of the glass and moving inward. For a borate glass, such as 13–93B3, the conversion is controlled by reaction at the interface and the kinetics can be described by a 3-D contracting sphere model. On the other hand, the conversion of a silicate glass, such as 13–93, is controlled initially by reaction at the interface (3-D contracting sphere model) and later by diffusion of ions to the reaction interface (3-D diffusion model).

If the reaction time is sufficiently long for the product to crystallize, the X-ray diffraction pattern of the converted materials often shows peaks that correspond to a reference HA, $Ca_{10}(PO_4)_6(OH)2$ [56,57,65,66]. However, microchemical analysis by energy-dispersive X-ray spectroscopy methods, for example, often shows a calcium-deficient HA in which the Ca/P atomic ratio is lower than 1.67, the value for a reference (or stoichiometric) HA. Furthermore, the Ca/P ratio of the converted material often varies from the surface of the reacted glass to the interior. Chemically, Fourier transform infrared spectra of the reacted material often show resonances attributable to carbonate $(CO_3)^{2-}$ groups [56,57,65,66]. This

has generally been interpreted as indicating the formation of a carbonate-substituted HA, in which some of the $(PO_4)^{3-}$ ions in the HA are substituted by $(CO_3)^{2-}$, as a result of dissolved CO_2 in the aqueous phosphate solution. However, the presence of a fine second phase of $CaCO_3$ cannot be ruled out. Substitution of OH^- in HA by $(CO_3)^{2-}$ can also occur, mainly in synthetic non-aqueous systems (1000 °C), but not in aqueous systems (25–100 °C) or biological apatites [34].

6.2. Micro/nanostructure of glass conversion product

The product of the bioactive glass conversion commonly consists of a mesoporous structure of nanophase particles with a high surface area [127]. Macroscopically, depending on the bioactive glass composition, the product can be either partially converted, consisting of an HA layer and an unconverted core (typical for slower-reacting silicate glasses such as 45S5 and 13–93), or fully converted to HA (typical for faster reacting borate glasses such as 13–93B3). Since the amount of HA formed in a fully converted material is dependent on the amount of Ca in the starting glass, and since the conversion reaction is pseudomorphic, porous or hollow HA products can be formed [70,128–131] (Fig. 5).

Scanning electron microscopy (SEM) examination of the cross-sections of bioactive glass conversion products has shown that, in some studies, the microstructure is not homogeneous throughout the section [56,57]. Instead, a layered structure is observed (Fig. 6). As shown, this layered structure can sometimes be quite complex, depending on the composition of the starting glass. Commonly, the outermost (or surface) layer has the most compact packing or lowest porosity. The mechanism for the formation of this layered structure is unclear. A possible explanation is that the conversion reaction does not proceed in a continuous manner. Instead, it starts and stops, presumably depending on the concentration of the reacting ions from the glass and the solution.

6.3. Mechanical performance of bioactive glass scaffolds

A key property, particularly for scaffolds intended for the repair of loaded bone, is the mechanical response. As previously discussed, scaffolds should have mechanical properties comparable to those of the tissue to be replaced. Bone is generally classified into two types: cortical bone, also referred to as compact bone, and trabecular bone, also referred to as cancellous or spongy bone. Cortical bone, found primarily in the shaft of long bones and as the outer shell around trabecular bone, is much denser, with a porosity of 5–10% [132]. Trabecular bone, found at the end of long bones, in vertebrae and in flat bones such as the pelvis, is much more porous, with porosity in the range 50–90% [133]. The mechanical properties of bone vary between subjects, from one bone to another and within different regions of the same bone. The mechanical properties are also highly anisotropic, as a result of the oriented microstructure. However, based on the testing of large specimens, the compressive strength and elastic modulus of cortical bone have been reported in the range 100–150 MPa and 5–15 GPa, respectively, in the direction parallel to the orientation axis (long axis) [134–136]. The strength and modulus in the direction perpendicular to the long axis are typically 1.5–2 times lower. A wide range has been reported for the elastic modulus (0.1–5 GPa) and compressive strength (2–12 MPa) of trabecular bone [135,136].

The mechanical properties of porous scaffolds depend on the type of biomaterial, the microstructure and the fabrication method. Table 2 shows the compressive strength of bioactive glass scaffolds prepared by a variety of methods. This summary is not meant to be exhaustive but, rather, to indicate representative examples. Bioactive glass scaffolds prepared by methods such as polymer foam replication, gel-casting and sintering of particles or short fibers typically have strengths comparable to that of human trabecular bone.

Methods such as rapid prototyping and unidirectional freezing of suspensions have resulted in the creation of porous bioactive glass scaffolds with compressive strength and elastic modulus which are comparable to, or approach the values for, human cortical bone. These scaffolds have potential application in the regeneration of load-bearing bones. Fig. 7 compares the mechanical response of 13–93 bioactive glass scaffolds formed by a polymer foam replication technique [110], unidirectional freezing [111] and by freeze extrusion fabrication (FEF), a rapid prototyping method [119]. Scaffolds prepared by the polymer foam replication technique (porosity = 85%; pore size = 100–400 μm) initially show an elastic response, followed by several peaks and valleys in the stress–strain curve. These peaks and valleys may be related to progressive breaking of the solid glass struts in the "trabecular" structure and compaction of the sample. Conversely, the constructs prepared by uniaxial freezing (porosity = 50%; pore size = 60–80 μm) or by rapid prototyping (FEF) (porosity = 50%, pore size = 100–500 μm) show a typical brittle response, consisting of an elastic response followed by fracture.

6.4. Response of bioactive glass to cells

The composition of the bioactive active glass has a marked effect on its ability to support the proliferation and function of cells in vitro (Fig. 8). Silicate bioactive glasses (45S5 or 13–93), in the form of disks or porous scaffolds, are well known to support the proliferation and differentiated function of osteoblastic cells, such as murine MC3T3-E1 cells and MLO-A5 cells, during conventional in vitro cell culture [69,102]. In contrast, borate bioactive glasses, such as 45S5B3 and 13–93B3 (the borate equivalent of 45S5 and 13–93), have shown a markedly lower ability to support cell proliferation and function [77,81]. This has been explained to be a consequence of the faster degradation rate of the borate glass and to the toxicity of the boron released into the culture medium. Borate glass leads to higher pH value of the culture medium (Fig. 4). High concentrations of boron released from the rapidly degrading borate glass also result in high local concentrations of boron in the medium, particularly near the surface of the glass.

It has been shown that, either by creating a more "dynamic" culture condition in which the system is gently shaken to mix the medium or by pre-reacting the borate bioactive glass in an aqueous phosphate solution to convert a surface layer of the glass to HA, the ability of borate bioactive glass to support cell proliferation and differentiation can be improved [80]. However, as described below, scaffolds of the same borate bioactive glass (e.g. 13–93B3) appear to show no observable toxic effects when implanted in vivo.

7. In vivo characteristics of bioactive glass scaffolds

Particles and granules of silicate 45S5 bioactive glass, as described previously, have been shown to enhance new bone formation in vivo [88–90]. Recent work has compared the effect of the bioactive glass composition on its ability to support tissue ingrowth in vivo. Fu et al. [77] implanted scaffolds, with the same "trabecular" microstructure (Fig. 2c) but with different compositions (silicate 13–93, borosilicate 13–93B1, borate 13–93B3), subcutaneously in the dorsum of rats, and evaluated the microstructure, microchemistry and histology of the scaffolds 6 weeks post-implantation. The scaffolds were found to convert faster to an HA-like material with increasing B_2O_3 content of the glass: both the borate 13–93B3 and borosilicate 13–93B1 were fully converted to HA, whereas the silicate 13–93 scaffold was only partially converted. This conversion in vivo, as a function of bioactive glass composition, is similar qualitatively to the conversion observed in vitro [77]. In contrast to the in vitro behavior, in which the borate glass showed a lower ability to support cell proliferation and function, all three groups of scaffolds showed the ability to support tissue infiltration during the six-week implantation.

Bi et al. [95] implanted scaffolds with a "fibrous" microstructure (Fig. 2b) and the same three compositions (13–93, 13–93B1, 13–93B3) for up to 12 weeks in a non-healing rodent calvaria defect model, and evaluated the ability of the scaffolds to support new bone formation and heal the defect. Defects filled with particles of silicate 45S5 bioactive glass (150–300 μm) and empty defects were used as positive and negative controls, respectively. The results showed that new bone formation was markedly dependent on the composition of the bioactive glass scaffolds. Fig. 9 shows hematoxylin and eosin (H&E)- and von Kossa-stained sections of silicate 13–93 and borate 13–93B3 scaffolds after the 12-week implantation. While all three scaffolds integrated well with the surrounding bone, a greater amount of the 13–93B3 scaffolds was converted to an HA-like material and a larger amount of new bone was formed within the 13–93B3 scaffolds. The borate 13–93B3 scaffolds were completely converted to HA, and some fibers developed a hollow core in which new tissue had infiltrated. Quantitative histomorphometric analysis showed that new bone formation in the borate 13–93B3 scaffolds (~15%) after the 12-week implantation was almost twice that for the silicate 13–93 scaffolds (Fig. 10). As a comparison, approximately half the size of a critical defect in bone will heal over time in a rodent model without the implantation of a scaffold.

In addition to the composition, the microstructure can also have an effect on the ability of the bioactive glass scaffold to support new tissue formation. When implanted subcutaneously for 4 weeks in the dorsum of rats, 13–93 bioactive glass scaffolds with an oriented microstructure (porosity = 60%; pore diameter = 90–110 μm) (Fig. 2c) showed a larger amount of tissue infiltration than "trabecular" scaffolds of the same glass (porosity = 85%; pore size = 100–500 μm) (Fig. 2b), despite the higher porosity and larger pore size of the "trabecular" scaffolds [112]. The reasons for the enhanced tissue infiltration in the oriented scaffolds are not clear. In a previous study [137], oriented poly(L-lactic acid) (PLLA) scaffolds showed a better ability to support in vitro osteoblastic cell growth and the formation of neo-tissue when compared to PLLA scaffolds with the same porosity but with a random 3-D pore architecture. This enhanced neo-tissue formation in the oriented scaffolds was attributed to the improved mass transport and/or cell–cell interaction. Furthermore, the importance of pore orientation on the in vitro and in vivo performance of scaffolds is well recognized in axonal and nerve regeneration [138,139]. However, differences in the surface roughness could also contribute to the amount of soft tissue infiltrated into the trabecular and oriented bioactive scaffolds.

Seeding with mesenchymal stem cells (MSCs) has also been found to enhance tissue infiltration into bioactive glass scaffolds. In one study [112], "trabecular" 13–93 bioactive glass scaffolds were seeded with rat bone marrow-derived MSCs, and implanted subcutaneously in the dorsum of rats for 4 weeks. The as-prepared 13–93 bioactive glass scaffolds (i.e. without MSCs) were used as a control. Histological evaluation (toluidine blue, Goldner's trichrome) showed that the amount of tissue infiltrated into the MSC-seeded scaffolds was approximately three times that for the unseeded scaffolds.

Despite the promising characteristics of borate bioactive glass for bone regeneration, as described above, the toxicity of the boron in vivo has been a concern, in view of the common observation that boron concentrations above a threshold value can be toxic to cells in vitro and in vivo [81,140]. Histological evaluation showed no adverse effects resulting from the implantation of borate bioactive glass (13–93B3) subcutaneously in the dorsum of rats [77,101] or in the calvaria of rats [95].

Further evaluation of borate 13–93B3 bioactive glass scaffolds in a rat subcutaneous implantation model showed that the bioactive borate glass caused no tissue damage to the kidney or the liver [82]. Five groups of rats (Sprague–Dawley) were evaluated: animals

implanted with 4, 8, 12 and 16 scaffolds (n = 4 per group), plus the control group (no implantation with borate bioactive glass scaffolds). Scaffolds with a "fibrous" microstructure (Fig. 2b), each with a mass of 70 mg, were implanted for 4 weeks. Based on previous subcutaneous implantation experiments, this implantation time was long enough for the scaffolds to completely react and convert to an HA-like material in vivo. After the animals were sacrificed, a kidney and a lobe of the liver were removed from each animal, and sections of each organ were cut and stained with H&E. The sections were sent for a blinded histological evaluation to Charles River Labs LLC (Shrewsbury, MA, USA), a commercial company that provides research and laboratory animal support services. No negative histological findings were found in the liver of any group, while the kidney had only minor incidental changes often seen in adult rats. Based on these toxicology results, borate bioactive glasses are non-toxic in the dynamic body environment of small animals, so they could be considered to be promising candidate materials for tissue regeneration in vivo.

The treatment of chronic osteomyelitis (bone infection) remains a clinical challenge. When loaded with the antibiotic teicoplanin, implants of borate bioactive glass showed promising results for treating osteomyelitis in a rabbit tibia model [80]. In that work, osteomyelitis was induced by methicillin-resistant *Staphylococcus aureus* (MRSA) in the rabbit tibia. After debridement, the bone cavity was filled with chitosan-bonded pellets of borate glass particles and teicoplanin powder. By 12 weeks post-implantation, the bioactive glass had converted to a bone-like HA graft and supported new bone ingrowth into the tibia defects (Fig. 11a–c). Furthermore, microbiological, histological and scanning electron microscopy techniques showed that the implants provided a cure for the bone infection. In comparison, animals treated with intravenous injection of teicoplanin for 4 weeks showed serious infection and a large amount of fibrosis after 12 weeks (Fig. 11d and e), indicating that intravenous teicoplanin was not effective for curing the infection.

Evaluation of the explants 12 weeks post-implantation using synchrotron X-ray microcomputed tomography (SR microCT) showed good osteoconduction and osteointegration of the bioactive glass implants in the bone cavity [141]. Three-dimensional reconstruction of the tibia cavity showed new trabecular bone formed in the cavity implanted with teicoplanin-loaded bioactive glass (Fig. 12a and b), but not in the empty defects (Fig. 12c and d) or in the cavity implanted with teicoplanin-loaded $CaSO_4$ (not shown). SR microCT also showed the infiltration of vascular tissue in the bioactive glass graft and in the newly formed trabecular bone. These results indicate that the combination of a borate bioactive glass and appropriate drugs could provide an effective method for treating osteomyelitis.

8. Bioactive glass in angiogenesis and soft tissue repair

While bioactive glasses have been extensively investigated for bone repair and regeneration, there has been relatively little research on the application of bioactive glasses to the repair or regeneration of soft tissues. However, recent work has shown the ability of bioactive glass to promote angiogenesis (formation of blood vessels), which is critical to numerous applications in tissue regeneration and the healing of soft tissue wounds.

Recent attempts to stimulate angiogenesis have focused on the delivery of growth factors, such as vascular endothelial growth factor (VEGF) and basic fibroblast growth factor (bFGF), gene therapy and cell-based therapy [142]. However, growth factors are expensive, and the optimal delivery strategies are unclear. The ability of a bioactive glass to induce angiogenesis could provide a robust alternative approach to the use of expensive growth factors for stimulating neovascularization of engineered tissues.

The beneficial effects of small concentrations of 45S5 bioactive glass for stimulating angiogenesis has been shown in several recent studies, as reviewed recently [143]. Polystyrene surfaces coated with a low concentration (0.01–0.2 wt.%) of silicate 45S5 bioactive glass particles (<5 μm) were found to enhance the proliferation of fibroblast 208F cells during in vitro culture for 24 h, when compared to the uncoated surfaces [144]. Culture medium collected from fibroblasts grown for 24 h on surfaces coated with 0.01 wt.% 45S5 glass contained significantly higher concentrations of VEGF. Furthermore, coating poly(glycolic acid) meshes with 45S5 glass was found to enhance neovascularization after subcutaneous implantation of the scaffolds in rats for 28 and 42 days.

Human fibroblasts encapsulated in alginate beads with specific quantities (0–1 wt.%) of silicate 45S5 bioactive glass particles (average size = 4 μm) secreted larger quantities of VEGF for bioactive glass concentrations of 0.01 and 0.1 wt.%, but not for 1.0 wt.%, indicating a dose-dependent curve for VEGF production which was dependent on the concentration of loaded material [145]. Furthermore, conditioned medium collected from the cell-seeded alginate beads containing 0.1 wt.% 45S5 glass particles increased endothelial cell proliferation. Human fibroblasts cultured on tissue culture surfaces coated with 45S5 glass particles (<5 μm) secreted larger amounts of VEGF and bFGF, while conditioned medium from the stimulated fibroblasts increased endothelial cell proliferation and tubule formation [146].

Coating a VEGF-releasing biodegradable PLGA scaffold with 45S5 bioactive glass particles resulted in an increase in endothelial cell proliferation in vitro, as well as greater neovascularization in vivo when implanted for 2 weeks in critical size defects in the cranium of Lewis rats [147]. By loading varying amounts of 45S5 bioactive glass into absorbable collagen sponges, the proangiogenic potential of 45S5 bioactive glass was shown to be related to the soluble products of the glass dissolution and the subsequent secretion of at least one angiogenic induction factor (VEGF) by the stimulated cells (Fig. 13) [148]. Furthermore, the proangiogenic potential of the bioactive glass was dose dependent, as observed previously [145]. In vivo, collagen sponges loaded with the optimum amount of 45S5 bioactive glass were found to enhance neovascularization 2 weeks post-implantation in irradiated calvaria defects of Sprague–Dawley rats, when compared to the collagen sponge without bioactive glass (control) [149]. This neovascularization induced by the local delivery of bioactive glass was believed to be responsible for the significantly greater new bone formation observed in the collagen/bioactive glass scaffolds 4 and 12 weeks post-implantation.

In addition to silicate 45S5 glass, other bioactive glasses are under investigation for their ability to promote angiogenesis. In a recent study [101], borate bioactive glass (13–93B3) scaffolds have shown promising results for promoting angiogenesis in a rat subcutaneous implantation model. Six weeks post-implantation, histomorphometric analysis of periodic acid–Schiff (PAS)-stained sections was used to evaluate the formation of blood vessels in the borate glass scaffolds (Fig. 14a). Red blood cells are stained light green, and can be seen in the center of many of the blood vessels (indicated by the arrows). The material from the original glass fibers of the scaffold is stained purple and labeled F, while soft tissue is stained a light blue color. As described earlier, some borate 13–93B3 glass fibers can develop a hollow core after conversion to an HA-like material. The scaffold section in Fig. 14b shows an H&E-stained section in which a fiber was cut perpendicular to the longitudinal fiber axis. The fiber reacted with the body fluids, converted to an HA-like material, and became filled with tissue and blood vessels (arrow). Fig. 14c shows a PAS-stained section in which a fiber was cut along the longitudinal axis; a blood vessel penetrated the hollow fiber and grew down the hollow core (arrow).

A direct role of copper to promote angiogenesis has been known for nearly three decades [150,151]. Copper (II) ions have been reported to stimulate the proliferation of endothelial cells in a dose-dependent manner during in vitro culture [152], and the ability of Cu ions to promote wound healing in rats has been linked to the up-regulation of VEGF by stimulated cells [153,154]. These findings suggest promising new strategies for the use of bioactive glass and other biomaterials to promote the desired vascularity in engineered tissues.

One approach is to exploit the compositional flexibility of glass, so that the bioactive glass is the source of the Cu required for enhancing angiogenesis. As the bioactive glass degrades and converts to an HA-like material, the Cu is released at the desired rate. “Fibrous” scaffolds (Fig. 2b) of borate bioactive glass (13–93B3) doped with varying amounts of Cu (0–1 wt.%) have recently been investigated to determine their ability to promote angiogenesis in a rat subcutaneous implantation model [101]. One group of scaffolds was seeded with rat bone marrow-derived MSCs, while the other group consisted of the as-prepared scaffolds (unseeded). Six weeks post-implantation, quantitative histomorphometric analysis of PAS stained blood vessels was used to evaluate the scaffolds (Fig. 15). As shown, borate bioactive glass scaffolds seeded with MSCs or doped with 0.4 wt.% Cu, or a combination of both (MSCs + 0.4 wt.% Cu), produced a significant increase in blood vessels compared to the as-prepared 13–93B3 scaffolds.

9. Bioactive glasses in chondrogenesis and osteochondral tissue engineering

While the ability of bioactive glass to promote osteogenesis is well known, recent work has shown that the soluble products of bioactive glass degradation may also promote neocartilage formation in vitro. When co-cultured with bovine chondrocyte-seeded agarose hydrogels, porous scaffolds of a silicate 13–93 bioactive glass served as a medium supplement for culturing tissue-engineered cartilage in vitro [155,156]. Constructs were cultured in serum-free, chemically defined medium supplemented with TGF-β 3 (10 ng ml^{-1} for the first 14 days of culture) [157]. Two studies were performed to evaluate short-term (2 weeks) vs. long-term (6 weeks) effects of exposing the cell-seeded hydrogels to bioactive glass (Fig. 16). In study 1, bioactive glass scaffolds were introduced to the culture medium of agarose hydrogels on day 28 of culture, and mechanical and biochemical changes were evaluated at 7 and 14 days after exposure. In study 2, bioactive glass scaffolds were added to the culture medium immediately after cell encapsulation. The glass scaffolds were removed after 14 days, the medium was replaced and the agarose hydrogels were cultured for a further 4 weeks. Agarose hydrogels maintained in normal culture medium without bioactive glass or cultured continuously with bioactive glass for the entire culture period (6 weeks) served as controls.

Mechanical testing of the agarose constructs was performed in unconfined compression, as described elsewhere [158]. After an initial tare load of 0.02 N, samples were loaded at a strain rate of 0.05% s^{-1} to a strain of 10% to measure the elastic modulus (E_Y). The dynamic modulus (G^*) was measured by superimposing a 2% peak-to-peak sinusoidal strain at 0.1 Hz. The constructs were digested in proteinase-K, and the glycosaminoglycan (GAG) and collagen contents were determined and normalized to the tissue net weight [159].

Transient exposure of the agarose hydrogels to bioactive glass scaffolds resulted in higher mechanical and biochemical properties than control samples (Fig. 17). In study 1, an immediate rise in properties was seen after 7 days of exposure, with a further increase by day 14. In study 2, significant increases in properties for constructs exposed transiently to bioactive glass construct occurred by day 42. Peak construct values achieved in this study were E_Y = 743 kPa, G^* = 2.8 MPa, GAG = 7.6 wt.% and collagen = 6.2 wt.%. These values

compare favorably with native bovine wrist cartilage [158]. The histology of transverse slides showed more rapid and homogeneous extracellular matrix distribution for constructs exposed to bioactive glass on day 28 (Fig. 18). Von Kossa stains for mineralization showed no difference from control slides.

The effect of bioactive glass was observed only with transient exposure (2 weeks), suggesting that there may be an optimum exposure time associated with these effects. Since an immediate effect of the exposure to bioactive glass was observed in study 1, and a delayed effect was observed in study 2 (weeks after exposure), the amount of elaborated matrix present in the agarose hydrogel may be an important modulator in the observed response to bioactive glass. One possible explanation is that, as the glass degrades in the culture medium, its ionic degradation products act as supplements to the medium that promote neocartilage tissue formation by modulating chondrocyte biosynthesis. These results suggest potential benefits of 13–93 bioactive glass on chondral tissue formation in engineered cartilage, in view of the well-known difficulty of regenerating cartilage and the limited ability of engineered cartilage to achieve the mechanical and biochemical properties of native cartilage [160].

Full-thickness articular cartilage defects often involve damage to the subchondral bone. Furthermore, bone-to-bone interfaces are known to integrate better and faster than cartilage-to-bone interfaces [161]. Tissue-engineered osteochondral grafts are therefore widely regarded as one of the most promising techniques for repairing full-thickness articular cartilage defects [162]. Numerous attempts have been made to develop cartilage–bone bilayered grafts using multi-material strategies and a variety of methods [16]. Despite several investigations examining the in vivo outcomes of tissue-engineered osteochondral grafts, the effect of the subchondral support material on graft integration and cell survival remains unclear.

Recent in vivo work has shown promising results for the use of silicate 13–93 bioactive glass as a suitable substrate for tissue-engineered osteochondral grafts [163]. Cylindrical plugs (3 mm in diameter × 6 mm) were made by bonding PEG hydrogel to three materials: porous 13–93 glass, porous tantalum metal and rabbit allograft bone. The empty defect was used a control. Chondrogenic-differentiated MSCs obtained from adult rabbit (New Zealand white) allogenic bone marrow were suspended in the 1 mm thick hydrogel cap and bonded to the three substrate materials before implantation into experimental defects in rabbit knees. Examination at 6 and 12 weeks post-implantation showed that both 13–93 glass and tantalum bonded to living bone, and supported viable cartilage cells at the articular layer. Osseointegration of the glass and tantalum was superior to allograft (Fig. 19), and transplanted cells expressed collagen type II collagen at 12 weeks post-implantation (Fig. 20).

10. Summary and future directions

While silicate bioactive glasses based on the 45S5 composition have been widely investigated over the last 40 years, recently developed bioactive glasses based on borate and borosilicate compositions are providing new opportunities for the application of bioactive glass in tissue engineering. Concerns about the toxicity of borate glasses to cells and tissues have been alleviated by results showing that borate glasses are non-toxic in small animals. Furthermore, while the ability of bioactive glass to support osteogenesis is well known, recent work has shown the proangiogenic potential of bioactive glass, which should provide benefits for the application of bioactive glass to soft tissue repair.

Despite its brittleness, bioactive glass has a unique set of properties, such as the ability to degrade at a controllable rate and convert to an HA-like material, to bond firmly to hard and

soft tissues, and to release ions during the degradation process. These ions are known to have a beneficial effect on osteogenesis and on angiogenesis, and recent results indicate that they may also have a beneficial effect on chondrogenesis. Future research will take advantage of the beneficial properties of bioactive glass, while seeking to limit the effects of its brittleness through innovative scaffold design and processing, particularly when applied to the repair of load-bearing bones.

Acknowledgments

This work was supported by the National Institutes of Health, National Institute of Arthritis and Musculoskeletal and Skin Diseases (NIH/NIAMS) Grant No. 1R15AR056119 (M.N.R., B.S.B.), the National Institute of Dental and Craniofacial Research (NIH/NIDCR) Grant No. 1R15DE018251 (M.N.R., D.E.D.) and the US Army Medical Research Acquisition Activity Contract No. W81XWH-08-1-0765 (M.N.R., D.E.D., L.F.B.). Q.F. and A.P.T. are grateful for the support from the National Institutes of Health/National Institute of Dental and Craniofacial Research (NIH/NIDCR) Grant No. 1R01DE015633. The authors thank Dr. R.F. Brown (Missouri S&T), Dr. J.L. Cook and Dr. P.K. Jayabalan (University of Missouri-Columbia), and Dr. C.T. Hung (Columbia University), for their collaboration.

Appendix A. Figures with essential colour discrimination

Certain figures in this article, particularly Figures 2, 4, 7, 9, 12, and 14–20, are difficult to interpret in black and white. The full colour images can be found in the on-line version, at doi:10.1016/j.actbio.2011.03.016.

References

1. Nerem RM. Cellular engineering. Ann Biomed Eng. 1991; 19:529–545. [PubMed: 1741530]
2. Langer R, Vacanti JP. Tissue engineering. Science. 1993; 260:920–926. [PubMed: 8493529]
3. Elisseeff J, McIntosh W, Fu K, Blunk R, Langer R. Controlled-release of IGF-I and TGF-β 1 in a photopolymerizing hydrogel for cartilage tissue engineering. J Orthop Res. 2001; 19:1098–1104. [PubMed: 11781011]
4. Babensee JE, McIntire LV, Mikos AG. Growth factor delivery for tissue engineering. Pharmaceut Res. 2000; 17:497–504.
5. Shea LD, Smiley E, Bonadio J, Mooney DJ. DNA delivery from polymer matrices for tissue engineering. Nat Biotechnol. 1999; 17:551–554. [PubMed: 10385318]
6. Mahoney MJ, Saltzman WM. Transplantation of brain cells assembled around a programmable synthetic microenvironment. Nat Biotechnol. 2001; 19:934–939. [PubMed: 11581658]
7. Cooper ML, Hansbrough JF. Use of a composite skin graft composed of cultured human keratinocytes and fibroblasts and a collagen–GAG matrix to cover full-thickness on athymic mice. Surgery. 1991; 109:198–207. [PubMed: 1992553]
8. Hansbrough JF, Morgan J, Greenleaf G, Parikh M, Nolte C, Wilkins L. Evaluation of Graftskin* composite grafts on full-thickness wounds on athymic mice. J Burn Care Rehabil. 1994; 15:346–353. [PubMed: 7929517]
9. Eaglstein WH, Falanga V. Tissue engineering and the development of Apligraf®, a human skin equivalent. Clin Ther. 1997; 19:894–905. [PubMed: 9385478]
10. Black AF, Berthod F, L'Heureux N, Germain L, Auger FA. In vitro reconstruction of a human capillary-like network in a tissue-engineered skin equivalent. FASEB J. 1998; 12:1331–1340. [PubMed: 9761776]
11. Vacanti CA, Bonassar LJ, Vacanti MP, Shufflebarger J. Replacement of an avulsed phalanx with tissue-engineered bone. N Eng J Med. 2001; 344:1511–1514.
12. Kruyt MC, van Gaalen SM, Oner FC, Verbout AJ, deBruijn JD, Dhert WJA. Bone tissue engineering and spinal fusion: the potential of hybrid constructs by combining osteoprogenitor cells and scaffolds. Biomaterials. 2004; 25:1463–1473. [PubMed: 14697849]

13. Marcacci M, Kon E, Moukhachev V, Lavroukov A, Kutepov S, Quarto R, et al. Stem cells associated with macroporous bioceramics for long bone repair: 6- to 7-year outcome of a pilot clinical study. Tissue Eng. 2007; 13:947–955. [PubMed: 17484701]
14. Cao Y, Vacanti JP, Paige KT, Upton J, Vacanti CA. Transplantation of chondrocytes utilizing a polymer-cell construct to produce tissue- engineered cartilage in the shape of a human ear. Plastic Reconstr Surg. 1997; 100:297–302.
15. Valonen PK, Moutos FT, Kusanagi A, Moretti MG, Diekman BO, Welter JF, et al. In vitro generation of mechanically functional cartilage grafts based on adult human stem cells and 3-D-woven poly(ε-caprolactone) scaffolds. Biomaterials. 2010; 31:2193–2200. [PubMed: 20034665]
16. Rahaman MN, Mao JJ. Stem cell-based composite tissue constructs for regenerative medicine. Biotechnol Bioeng. 2005; 91:261–284. [PubMed: 15929124]
17. Hutmacher DW. Scaffold design and fabrication technologies for engineering tissues - state of the art and future perspectives. J Biomater Sci: Polym Ed. 2001; 12:107–124. [PubMed: 11334185]
18. Griffith LG. Emerging design principles in biomaterials and scaffolds for tissue engineering. Ann NY Acad Sci. 2002; 961:83–95. [PubMed: 12081872]
19. Li WJ, Laurencin CT, Caterson EJ, Tuan RS, Ko FK. Electrospun nanofibrous structure: a novel scaffold for tissue engineering. J Biomed Mater Res. 2002; 60:613–621. [PubMed: 11948520]
20. Shin M, Yoshimoto H, Vacanti JP. In vivo bone tissue engineering using mesenchymal stem cells on a novel electrospun nanofibrous scaffold. Tissue eng. 2004; 10:33–41. [PubMed: 15009928]
21. Hollister SJ. Porous scaffold design for tissue engineering. Nat Mater. 2005; 4:518–524. [PubMed: 16003400]
22. Deville S, Saiz E, Tomsia A. Freeze casting of hydroxyapatite scaffolds for bone tissue engineering. Biomaterials. 2006; 27:5480–5489. [PubMed: 16857254]
23. Griffith LG. Polymeric biomaterials. Acta Mater. 2000; 48:263–277.
24. Agrawal CM, Ray RB. Biodegradable polymer scaffolds for musculoskeletal tissue engineering. J Biomed Mater Res. 2001; 55:141–150. [PubMed: 11255165]
25. Hayashi T. Biodegradable polymers for biomedical uses. Prog Polym Sci. 1994; 19:663–702.
26. Reis, RL., editor. Natural-based polymers for biomedical applications. Cambridge: Woodhead Publishing; 2008.
27. Lee KY, Mooney DJ. Hydrogels for tissue engineering. Chem Rev. 2001; 101:1869–1878. [PubMed: 11710233]
28. Varghese S, Elisseeff JH. Hydrogels for musculoskeletal tissue engineering. Adv Polym Sci. 2006; 203:95–144.
29. Thompson RC, Yaszemski MJ, Powers JM, Mikos AG. Hydroxyapatite fiber- reinforced poly(-hydroxy ester) foams for bone regeneration. Biomaterials. 1998; 19:1935–1943. [PubMed: 9863527]
30. Zhang R, Ma PX. Poly(α-hydroxyl acids)/hydroxyapatite porous composites for bone tissue engineering. I. Preparation and morphology. J Biomed Mater Res. 1999; 44:446–455. [PubMed: 10397949]
31. Lu HH, El-Amin SF, Scott KD, Laurencin CT. Three-dimensional, bioactive, biodegradable, polymer-bioactive glass composite scaffolds with improved mechanical properties support collagen synthesis and mineralization of human osteoblast-like cells in vitro. J Biomed Mater Res. 2003; 64A:465–474.
32. Kim S-S, Ahn KM, Park MS, Lee J-H, Choi CY, Kim B-S. A poly(lactide coglycolide)/hydroxyapatite composite scaffold with enhanced osteoconductivity. J Biomed Mater Res. 2007; 80A:206–215.
33. Witte F, Kaese V, Haferkamp H, Switzer E, Meyer-Lindenberg A, Wirth CJ, et al. In vivo corrosion of four magnesium alloys and the associated bone response. Biomaterials. 2005; 26:3557–3563. [PubMed: 15621246]
34. LeGeros, RZ.; LeGeros, JP. Phosphate minerals in human tissues. In: Nriagu, JO.; Moore, PB., editors. Phosphate minerals. Berlin: Springer-Verlag; 1984. p. 351-385.
35. Hench, LL.; Wilson, J., editors. An introduction to bioceramics. Singapore: World Scientific; 1993.

36. Gauthier O, Goyenvalle E, Bouler J, Guicheux J, Pilet P, Weiss P, et al. Macroporous biphasic calcium phosphate ceramics versus injectable bone substitute: a comparative study 3 and 8 weeks after implantation in rabbit bone. J Mater Sci Mater Med. 2001; 12:385–390. [PubMed: 15348276]
37. Bandyopadhyay A, Bernard S, Xue W, Bose S. Calcium phosphate-based resorbable ceramics: influence of MgO, ZnO, and SiO_2 dopants. J Am Ceram Soc. 2006; 89:2675–2688.
38. Klein C, Patka P, den Hollander W. Macroporous calcium phosphate bioceramics in dog femora: a histological study of interface and biodegradation. Biomaterials. 1989; 10:59–62. [PubMed: 2540845]
39. Martin RB, Chapman MW, Sharkey NA, Zissimos SL, Bay B, Shors EC. Bone ingrowth and mechanical properties of coralline hydroxyapatite 1 year after implantation. Biomaterials. 1993; 14:341–348. [PubMed: 8389612]
40. Daculsi G, Laboux O, Malard O, Weiss P. Current state of the art of biphasic calcium phosphate bioceramics. J Mater Sci Mater Med. 2003; 14:195–200. [PubMed: 15348464]
41. Wagoner Johnson AJ, Herschler BA. A review of the mechanical behavior of CaP and CaP/polymer composites for applications in bone replacement and repair. Acta Biomater. 2011; 7:16–30. [PubMed: 20655397]
42. Hench LL, Wilson J. Surface active biomaterials. Science. 1984; 226:630–636. [PubMed: 6093253]
43. Yamamuro, T.; Hench, LL.; Wilson, J., editors. Handbook of bioactive ceramics, vols. 1 and 2. Boca Raton, FL: CRC Press; 1990.
44. Hench LL. Bioceramics. J Am Ceram Soc. 1998; 81:1705–1728.
45. Rahaman MN, Brown RF, Bal BS, Day DE. Bioactive glasses for non-bearing applications in total joint replacement. Semin Arthroplasty. 2007; 17:102–112.
46. Williams, DF., editor. Definitions in biomaterials. New York: Elsevier; 1987.
47. Kokubo T, Takadama H. How useful is SBF in predicting in vivo bone bioactivity? Biomaterials. 2006; 27:2907–2915. [PubMed: 16448693]
48. Kokubo T, Kushitani H, Sakka S, Kitsugi T, Yamamuro T. Solutions able to reproduce in vivo surface-structure changes in bioactive glass-ceramic A-W. J Biomed Mater Res. 1990; 24:721–734. [PubMed: 2361964]
49. Ducheyne P. Bioceramics: materials characteristics versus in vivo behavior. J Biomed Mater Res. 1987; 21(A2 Suppl.):219–236. [PubMed: 3624287]
50. Bohner M, Lemaître J. Can bioactivity be tested in vitro with SBF solution? Biomaterials. 2009; 30:2175–2179. [PubMed: 19176246]
51. Ohura K, Bohner M, Hardouin P, Lemaître J, Pasquier G, Flautre B. Resorption of, and bone formation from, new β-tricalcium phosphate–monocalcium phosphate cements: an in vivo study. J Biomed Mater Res. 1996; 30:1993–2000.
52. Apelt D, Theiss F, El-Warrak AO, Zlinszky K, Bettschart-Wolfisberger R, Bohner M, et al. In vivo behavior of three different injectable hydraulic calcium phosphate cements. Biomaterials. 2004; 25:1439–1451. [PubMed: 14643619]
53. Theiss F, Apelt D, Brand B, Kutter A, Zlinszky K, Bohner M, et al. Biocompatibility and resorption of a brushite calcium phosphate cement. Biomaterials. 2005; 26:4383–4394. [PubMed: 15701367]
54. Kotani S, Fujita Y, Kitsugi T, Nakamura T, Yamamuro T, Ohtsuki C, et al. Bone bonding mechanisms of β -tricalcium phosphate. J Biomed Mater Res. 1991; 25:1303–1315. [PubMed: 1812121]
55. Hench LL, Splinter RJ, Allen WC, Greenlee TK Jr. Bonding mechanisms at the interface of ceramic prosthetic materials. J Biomed Mater Res. 1971; 5:117–141.
56. Huang W, Day DE, Kittiratanapiboon K, Rahaman MN. Kinetics and mechanisms of the conversion of silicate (45S5), borate, and borosilicate glasses to hydroxyapatite in dilute phosphate solution. J Mater Sci Mater Med. 2006; 17:583–596. [PubMed: 16770542]
57. Huang W, Rahaman MN, Day DE, Li Y. Mechanisms of converting silicate, borate, and borosilicate glasses to hydroxyapatite in dilute phosphate solution. Phys Chem Glasses Europ J Glass Sci Technol B. 2006; 47:647–658.

58. Rohanová D, Boccaccini AR, Yunos DM, Horhavková D, Březovska I, Helebrant A. TRIS buffer in simulated body fluid (SBF) distorts the assessment of glass-ceramic scaffold bioactivity. Acta Biomater. in press.
59. Hench LL, Polak JM. Third-generation biomaterials. Science. 2002; 295:1014–1017. [PubMed: 11834817]
60. Ducheyne P, Qiu Q. Bioactive ceramics: the effect of surface reactivity on bone formation and bone cell function. Biomaterials. 1999; 20:2287–2303. [PubMed: 10614935]
61. Wilson J, Pigott GH, Schoen FJ, Hench LL. Toxicology and biocompatibility of bioglasses. J Biomed Mater Res. 1981; 15:805–817. [PubMed: 7309763]
62. Lai W, Garino J, Ducheyne P. Silicon excretion from bioactive glass implanted in rabbit bone. Biomaterials. 2002; 23:213–217. [PubMed: 11762840]
63. Chen ZQ, Thompson ID, Boccaccini AR. 45S5 Bioglass®-derived glass-ceramic scaffold for bone tissue engineering. Biomaterials. 2006; 27:2414–2425. [PubMed: 16336997]
64. Filho OP, LaTorr GP, Hench LL. Effect of crystallization on apatite-layer formation on bioactive glass 45S5. J Biomed Mater Res. 1996; 30:509–514. [PubMed: 8847359]
65. Yao A, Wang DP, Huang W, Rahaman MN, Day DE. In vitro bioactive characteristics of borate-based glasses with controllable degradation behavior. J Am Ceram Soc. 2007; 90:303–306.
66. Fu Q, Rahaman MN, Fu H, Liu X. Bioactive glass scaffolds with controllable degradation rates for bone tissue engineering applications. I. Preparation and in vitro degradation. J Biomed Mater Res. 2010; 95A:164–171.
67. Brink M. The influence of alkali and alkali earths on the working range for bioactive glasses. J Biomed Mater Res. 1997; 36:109–117. [PubMed: 9212395]
68. Brink M, Turunen T, Happonen R, Yli-Urppo A. Compositional dependence of bioactivity of glasses in the system $Na_2O–K_2O–MgO–CaO–B_2O3–P_2O5–SiO_2$. J Biomed Mater Res. 1997; 37:114–121. [PubMed: 9335356]
69. Brown RF, Day DE, Day TE, Jung S, Rahaman MN, Fu Q. Growth and differentiation of osteoblastic cells on 13–93 bioactive glass fibers and scaffolds. Acta Biomater. 2008; 4:387–396. [PubMed: 17768097]
70. Day DE, White JE, Brown RF, McMenamin KD. Transformation of borate glasses into biologically useful materials. Glass Technol Part A. 2003; 44:75–81.
71. Day, DE.; Erbe, EM.; Richard, M.; Wojcik, JA. Bioactive materials. US Patent. No. 6709,744. 2004 March 23.
72. Han X, Day DE. Reaction of sodium calcium borate glasses to form hydroxyapatite. J Mater Sci Mater Med. 2007; 18:1837–1847. [PubMed: 17486301]
73. Zhao D, Huang W, Rahaman MN, Day DE, Wang DP. Mechanism for converting Al_2O_3-containing borate glass to hydroxyapatite in aqueous phosphate solution. Acta Biomater. 2009; 5:1265–1273. [PubMed: 19119086]
74. Pan H, Zhao X, Zhang X, Zhang K, Li L, Li Z, et al. Strontium borate glass: potential biomaterial for bone regeneration. J Roy Soc Interface. 2010; 7:1025–1031. [PubMed: 20031984]
75. Marion N, Liang W, Reilly G, Day DE, Rahaman MN, Mao JJ. Bioactive borate glass supports the osteogenic potential of human mesenchymal stem cells. Mech Adv Mater Struct. 2005; 12:239–246.
76. Fu H, Fu Q, Zhou N, Huang W, Rahaman MN, Wang D, et al. In vitro evaluation of borate-based bioactive glass scaffolds prepared by a polymer foam replication method. Mater Sci Eng C. 2009; 29:2275–2281.
77. Fu Q, Rahaman MN, Bal BS, Bonewald LF, Kuroki K, Brown RF. Bioactive glass scaffolds with controllable degradation rates for bone tissue engineering applications. II. In vitro and in vivo biological evaluation. J Biomed Mater Res. 2010; 95A:172–179.
78. Liu X, Xie Z, Zhang C, Pan H, Rahaman MN, Zhang X, et al. Bioactive borate glass scaffolds: in vitro and in vivo evaluation for use as a drug delivery system in the treatment of bone infection. J Mater Sci Mater Med. 2010; 21:575–582. [PubMed: 19830527]
79. Jia WT, Zhang X, Luo SH, Huang WH, Rahaman MN, Day DE, et al. Novel borate glass/chitosan composite as a delivery vehicle for teicoplanin in the treatment of chronic osteomyelitis. Acta Biomater. 2010; 6:812–819. [PubMed: 19770078]

80. Zhang X, Jia W, Gu Y, Liu X, Wang D, Zhang C, et al. Teicoplanin-loaded borate bioactive glass implants for treating chronic bone infection in a rabbit tibia osteomyelitis model. Biomaterials. 2010; 31:5865–5874. [PubMed: 20434766]
81. Brown RF, Rahaman MN, Dwilewicz AB, Huang W, Day DE, Li Y, et al. Conversion of borate glass to hydroxyapatite and its effect on proliferation of MC3T3-E1 cells. J Biomed Mater Res. 2009; 88A:392–400.
82. Jung SB, Day DE, Brown RF, Bonewald LF. Potential toxicity of bioactive borate glasses in vitro and in vivo, submitted for publication.
83. Uo M, Mizuno M, Kukobi Y, Makishima A, Watari F. Properties and cytotoxicity of water-soluble $Na_2O{-}CaO{-}P_2O_5$ glasses. Biomaterials. 1998; 19:2277–2284. [PubMed: 9884040]
84. Franks K, Abrahams I, Knowles JC. Development of soluble glasses for biomedical use. Part I. In vitro solubility measurement. J Mater Sci Mater Med. 2000; 11:609–614. [PubMed: 15348084]
85. Salih V, Franks K, James M, Hastings GW, Knowles JC, Olsen I. Development of soluble glasses for biomedical use. Part II. The biological response of human osteoblast cell lines to phosphate-based soluble glasses. J Mater Sci Mater Med. 2000; 11:615–620. [PubMed: 15348085]
86. Ahmed I, Lewis M, Olsen I, Knowles JC. Phosphate glasses for tissue engineering. Part 1. Processing and characterization of a ternary-based $P2O_5{-}CaO{-}Na_2O$ glass system. Biomaterials. 2004; 25:491–499. [PubMed: 14585698]
87. Ahmed I, Lewis M, Olsen I, Knowles JC. Phosphate glasses for tissue engineering. Part 2. Processing and characterization of a ternary-based $P2O_5{-}CaO{-}Na_2O$ glass fiber system. Biomaterials. 2004; 25:501–507. [PubMed: 14585699]
88. Wheeler DL, Stokes KE, Park HM, Hollinger JO. Evaluation of particulate Bioglass® in a rabbit radius ostectomy model. J Biomed Mater Res. 1997; 35:249–254. [PubMed: 9135173]
89. Wheeler DL, Stokes KE, Hoellrich RG, Chamberlain DL, McLoughlin SW. Effect of bioactive glass particle size on osseous regeneration of cancellous defects. J Biomed Mater Res. 1998; 41:527–533. [PubMed: 9697024]
90. Oonishi H, Hench LL, Wilson J, Sugihara F, Tsuji E, Kushitani S, et al. Comparative bone growth behavior in granules of bioceramic materials of various sizes. J Biomed Mater Res. 1999; 44:31–43. [PubMed: 10397902]
91. Xynos ID, Hukkanen MVJ, Batten JJ, Buttery LD, Hench LL, Polak JM. Bioglass® 45S5 stimulates osteoblast turnover and enhances bone formation in vitro: implications and applications for bone tissue engineering. Calcif Tissue Int. 2000; 67:321–329. [PubMed: 11000347]
92. Xynos ID, Edgar AJ, Buttery LDK, Hench LL, Polak JM. Ionic products of bioactive glass dissolution increase proliferation of human osteoblasts and induce insulin-like growth factor II mRNA expression and protein synthesis. Biochem Biophys Res Comm. 2000; 276:461–465. [PubMed: 11027497]
93. Xynos ID, Edgar AJ, Buttery LDK, Hench LL, Polak JM. Gene-expression profiling of human osteoblasts following treatment with the ionic products of Bioglass® 45S5 dissolution. J Biomed Mater Res. 2001; 55:151–157. [PubMed: 11255166]
94. Bohner M. Silicon-substituted calcium phosphates - a critical review. Biomaterials. 2009; 30:6403–6406. [PubMed: 19695699]
95. Bi L, Jung SB, Day DE, Neidig K, Dusevich V, Eick D, et al. Evaluation of bone regeneration, angiogenesis, and hydroxyapatite conversion in critical-sized rat calvarial defects implanted with bioactive glass scaffolds. in preparation.
96. Hulbert SF, Young FA, Mathews RS, Klawitter JJ, Talbert CD, Stelling FH. Potential of ceramic materials as permanently implantable skeletal prostheses. J Biomed Mater Res. 1970; 4:433–456. [PubMed: 5469185]
97. Hollinger JO, Brekke J, Gruskin E, Lee D. Role of bone substitutes. Clin Orthop Relat Res. 1996; 324:55–65. [PubMed: 8595778]
98. Pirhonen E, Moimas L, Haapanen J. Porous bioactive 3-D glass fiber scaffolds for tissue engineering applications manufactured by sintering technique. Key Eng Mater. 2003; 240–242:237–240.

99. Fu Q, Rahaman MN, Bal BS, Huang W, Day DE. Preparation and bioactive characteristics of a porous 13–93 glass, and fabrication into the articulating surface of a proximal tibia. J Biomed Mater Res. 2007; 82A:222–229.
100. Liang W, Rahaman MN, Day DE, Marion NW, Riley GC, Mao JJ. Bioactive borate glass scaffold for bone tissue engineering. J. Non-Crystalline Solids. 2008; 354:1690–1696.
101. Jung SB, Day DE, Brown RF. Angiogenic bioactive borate glasses. submitted for publication.
102. Fu Q, Rahaman MN, Bal BS, Brown RF, Day DE. Mechanical and in vitro performance of 13–93 bioactive glass scaffolds prepared by a polymer foam replication technique. Acta Biomater. 2008; 4:1854–1864. [PubMed: 18519173]
103. Liu X, Pan H, Fu H, Fu Q, Rahaman MN, Huang W. Conversion of borate-based glass scaffold to hydroxyapatite in dilute phosphate solution. Biomed Mater. 2010; 5:015005.
104. Wang HW, Tabata Y, Ikada Y. Fabrication of porous gelatin scaffolds for tissue engineering. Biomaterials. 1999; 20:1339–1344. [PubMed: 10403052]
105. Fukasawa T, Ando M, Ohji T, Kanzaki S. Synthesis of porous ceramics with complex pore structure by freeze-dry processing. J Am Ceram Soc. 2001; 84:230–232.
106. Schoof H, Apel J, Heschel I, Rau G. Control of pore structure and size in freeze-dried collagen sponges. J Biomed Mater Res Appl Biomater. 2001; 58:352–357.
107. Zhang H, Hussain I, Brust M, Butler MF, Rannard S, Cooper AI. Aligned two- and three-dimensional structures by directional freezing of polymers and nanoparticles. Nat Mater. 2005; 4:787–793. [PubMed: 16184171]
108. Fu Q, Rahaman MN, Dogan F, Bal BS. Freeze casting of porous hydroxyapatite scaffolds. I. Processing and general microstructure. J Biomed Mater Res. 2008; 86B:125–135.
109. Fu Q, Rahaman MN, Dogan F, Bal BS. Freeze casting of porous hydroxyapatite scaffolds. II. Sintering, microstructure, and mechanical behavior. J Biomed Mater Res. 2008; 86B:514–522.
110. Fu Q, Rahaman MN, Bal BS, Brown RF. Preparation and in vitro evaluation of bioactive glass (13–93) scaffolds with oriented microstructures for repair and regeneration of load-bearing bones. J Biomed Mater Res. 2010; 93A:1380–1390.
111. Liu X, Rahaman MN, Fu Q. Oriented bioactive glass (13–93) scaffolds with controllable pore size by unidirectional freezing of camphene-based suspensions: microstructure and mechanical response. Acta Biomater. 2011; 7:410–416.
112. Fu Q, Rahaman MN, Bal BS, Kuroki K, Brown RF. In vivo evaluation of 13–93 bioactive glass scaffolds with trabecular and oriented microstructures in a rat subcutaneous implantation model. J Biomed Mater Res. 2010; 95A:235–244.
113. Pham, DT.; Dimov, SS., editors. The technologies and applications of rapid prototyping and rapid tooling. London: Springer; 2000.
114. Sachlos E, Czernuszka JT. Making tissue engineering scaffolds work. Review of the application of solid freeform fabrication technology to the production of tissue engineering scaffolds. Eur Cells Mater. 2003; 5:29–40.
115. Chu, TMG. Solid freeform fabrication of tissue engineering scaffolds. In: Ma, PX.; Elisseeff, JH., editors. Scaffolding in tissue engineering. Boca Raton, FL: Taylor & Francis; 2005. p. 139-154.
116. Rezwan K, Chen QZ, Blaker JJ, Boccaccini AR. Biodegradable and bioactive porous polymer/inorganic composite scaffolds for bone tissue engineering. Biomaterials. 2006; 27:3413–3431. [PubMed: 16504284]
117. Russias J, Saiz E, Deville S, Tomsia AP. Fabrication and in-vitro characterization of three-dimensional composite scaffolds by robocasting for biomedical applications. Adv Sci Technol. 2006; 49:153–158.
118. Fu Q, Saiz E, Tomsia AP. Bio-inspired highly porous and strong glass scaffolds. Adv Funct Mater. in press.
119. Huang TS, Rahaman MN, Doiphode ND, Leu MC, Bal BS, Day DE. Porous and strong bioactive glass (13–93) scaffolds prepared by freeze extrusion fabrication. Mater Sci Eng C. submitted for publication.
120. Velez, M. SBIR/STTR Phase I Final Report. Rolla, MO: Corp.; 2010. Selective laser sintering of bioglass for bone tissue engineering.

121. Sepulveda P, Jones JR, Hench LL. Bioactive sol-gel foams for tissue repair. J Biomed Mater Res. 2002; 59:340–348. [PubMed: 11745571]
122. Jones JR, Poologasundarampillai G, Atwood RC, Bernard D, Lee PD. Nondestructive quantitative 3-D analysis for the optimization of tissue scaffolds. Biomaterials. 2007; 28:1404–1413. [PubMed: 17141863]
123. Jones JR, Ehrenfried LM, Hench LL. Optimizing bioactive glass scaffolds for bone tissue engineering. Biomaterials. 2006; 27:964–973. [PubMed: 16102812]
124. Kim H-W, Kim H-E, Knowles JC. Production and potential of bioactive glass nanofibers as a next-generation biomaterial. Adv Func Mater. 2006; 16:1529–1535.
125. Lu H, Zhang T, Wang XP, Fang QF. Electrospun submicron bioactive glass fibers for bone tissue scaffold. J Mater Sci Mater Med. 2009; 20:793–798. [PubMed: 19020952]
126. Jung SB, Day DE. Conversion kinetics of silicate, borosilicate, and borate bioactive glasses to hydroxyapatite. Phys Chem Glasses Eur J Glass Sci Technol B. 2009; 50:85–88.
127. Rahaman MN, Day DE, Brown RF, Fu Q, Jung SB. Nanostructured bioactive glass scaffolds for bone repair. Cer Eng Sci Proc. 2008; 29:211–225.
128. Conzone SD, Day DE. Preparation and properties of porous microspheres made form borate glass. J Biomed Mater Res. 2009; 88A:531–542.
129. Wang Q, Huang W, Wang D, Darvell BW, Day DE, Rahaman MN. Preparation of hollow hydroxyapatite microspheres. J Mater Sci Mater Med. 2006; 17:641–646. [PubMed: 16770549]
130. Huang W, Rahaman MN, Day DE, Miller BA. Strength of hollow hydroxyapatite microspheres prepared by a glass conversion process. J Mater Sci Mater Med. 2009; 20:123–129. [PubMed: 18704649]
131. Fu H, Rahaman MN, Day DE, Fu Q. Effect of process parameters on the microstructure of hollow hydroxyapatite microspheres prepared by a glass conversion method. J Am Ceram Soc. 2010; 93:3116–3123.
132. Martin, RB.; Burr, DB.; Sharkey, NA. Skeletal tissue mechanics. New York: Springer-Verlag; 1998.
133. Goldstein SA. The mechanical properties of trabecular bone: dependence on anatomic location and function. J Biomech. 1987; 20:1055–1062. [PubMed: 3323197]
134. Reilly DT, Burstein AH, Frankel VH. The elastic modulus of bone. J Biomech. 1974; 7:271–275. [PubMed: 4846264]
135. Fung, YC. Biomechanics: mechanical properties of living tissues. New York: Springer; 1993.
136. Rho JY, Hobatho MC, Ashman RB. Relations of density and CT numbers to mechanical properties for human cortical and cancellous bone. Med Eng Phys. 1995; 17:347–355. [PubMed: 7670694]
137. Ma PX, Zhang R. Microtubular architecture of biodegradable polymer scaffolds. J Biomed Mater Res. 2001; 56:469–477. [PubMed: 11400124]
138. Stokols S, Tuszynski MH. Freeze-dried agarose scaffolds with uniaxial channels stimulate and guide linear axonal growth following spinal cord injury. Biomaterials. 2006; 27:443–451. [PubMed: 16099032]
139. Kim Y, Haftel VK, Kumar S, Bellamkonda RV. The role of aligned polymer fiber-based constructs in the bridging of long peripheral nerve gaps. Biomaterials. 2008; 29:3117–3127. [PubMed: 18448163]
140. Heindel JJ, Price CJ, Schwetz BA. The developmental toxicity of boric acid in mice, rats, and rabbits. Environ Health Perspect. 1994; 102:107–112. [PubMed: 7889869]
141. Fu Q, Huang W, Jia W, Rahaman MN, Liu X, Tomsia AP. Osteoconduction and osteointegration by bioactive borate glass in a rabbit tibia model: a synchrotron X-ray micro computerized tomography (SR microCT) study. submitted for publication.
142. Carmeliet P. Manipulating angiogenesis in medicine. J Intern Med. 2004; 255:538–561. [PubMed: 15078497]
143. Gorustovich AA, Perio C, Roether JA, Boccaccini AR. Effect of bioactive glasses on angiogenesis: a review of in vitro and in vivo evidence. Tissue Eng B. 2010; 16:199–207.

144. Day RM, Boccaccini AR, Shurey S, Roether JA, Forbes A, Hench LL, et al. Assessment of poly(glycolic acid) mesh and bioactive glass for soft tissue engineering scaffolds. Biomaterials. 2004; 25:5857–5866. [PubMed: 15172498]

145. Keshaw H, Forbes A, Day RM. Release of angiogenic growth factors from cells encapsulated in alginate beads with bioactive glass. Biomaterials. 2005; 26:4171–4179. [PubMed: 15664644]

146. Day RM. Bioactive glass stimulates the secretion of angiogenic growth factors and angiogenesis in vitro. Tissue Eng. 2005; 11:768–777. [PubMed: 15998217]

147. Leach JK, Kaigler D, Wang Z, Kresbach PH, Mooney DJ. Coating of VEGF- releasing scaffolds with bioactive glass for angiogenesis and bone regeneration. Biomaterials. 2006; 27:3249–3255. [PubMed: 16490250]

148. Leu A, Stieger SM, Dayton P, Ferrara KW, Leach JK. Angiogenic response to bioactive glass promotes bone healing in an irradiated calvarial defect. Tissue Eng Part A. 2008; 15:877–885. [PubMed: 18795867]

149. Leu A, Leach JK. Proangiogenic potential of a collagen bioactive glass substrate. Pharmaceut Res. 2008; 25:1122–1129.

150. McAuslan BR, Reilly. Endothelial cell phagokinesis in response to specific metal ions. Exp Cell Res. 1980; 130:147–157. [PubMed: 6161014]

151. Raju KS, Alessandri G, Ziche M, Gullino PM. Ceruloplasmin, copper ions, and angiogenesis. J Natl Cancer Inst. 1982; 69:1183–1188. [PubMed: 6182332]

152. Hu GF. Copper stimulates proliferation of human endothelial cells under culture. J Cell Biochem. 1998; 69:326–335. [PubMed: 9581871]

153. Sen CK, Khanna S, Venojarvi M, Trikha P, Ellison EC, Hunt TK, et al. Copper- induced vascular endothelial growth factor expression and wound healing. Am J Physiol Heart Circ Physiol. 2002; 282:H1821–H1827. [PubMed: 11959648]

154. Frangoulis M, Georgiou P, Chrisostomidis C, Perrea D, Dontas I, Kavantzas N, et al. Rat epigastric flap survival and VEGF expression after local copper application. Plast Reconstr Surg. 2007; 119:837–843. [PubMed: 17312485]

155. Tan, AR.; Barsi, JM.; Jayabalan, PS.; Rahaman, MN.; Bal, BS.; Ateshian, GA., et al. Bioactive glass as a medium supplement for culturing tissue-engineered cartilage. Transactions of the 55th Annual Meeting of the Orthopaedic Research Society; Las Vegas, NV. 2009. p. 1314

156. Jayabalan PS, Tan AR, Rahaman MN, Bal BS, Hung CT, Cook JL. Bioactive glass (13–93) as a subchondral substrate for tissue-engineered osteochondral constructs. Clin Orthop Rel Res. in press.

157. Lima EG, Bian L, Ng KW, Mauck RL, Byers BA, Tuan RS, et al. The beneficial effect of delayed compressive loading on tissue-engineered cartilage constructs cultured with TGF-β 3. Osteoarthritis Cartilage. 2007; 15:1025–1033. [PubMed: 17498976]

158. Lima EG, Tan AR, Tai T, Bian L, Stoker AM, Ateshian GA, et al. Differences in interleukin-1 response between engineered and native cartilage. Tissue Eng Part A. 2008; 14:1721–1730. [PubMed: 18611148]

159. Kelly TA, Ng KW, Wang CC, Ateshian GA, Hung CT. Spatial and temporal development of chondrocytes-seeded agarose constructs in free-swelling and dynamically loaded cultures. J Biomech. 2006; 39:1489–1497. [PubMed: 15990101]

160. Hunziker EB. The elusive path to cartilage regeneration. Adv Mater. 2009; 21:3419–3424. [PubMed: 20882507]

161. Hunziker EB. Articular cartilage repair: basic science and clinical progress. A review of current status and prospects. Osteoarthritis Cartilage. 2001; 10:432–463. [PubMed: 12056848]

162. Freed LE, Engelmayr GC Jr, Borenstein JT, Moutos FT, Guilak F. Advanced material strategies for tissue engineering scaffolds. Adv Mater. 2009; 21:3410–3418. [PubMed: 20882506]

163. Bal BS, Rahaman MN, Jayabalan PS, Kuroki K, Cockrell Mary K, Yao JQ, et al. In vivo outcomes of tissue-engineered osteochondral grafts. J Biomed Mater Res. 2010; 93B:164–174.

164. Liu X, Rahaman MN, Fu Q. Effect of cooling rate on pore orientation and mechanical strength of 13–93 bioactive glass scaffolds prepared by unidirectional freezing of camphene-based suspensions. submitted for publication.

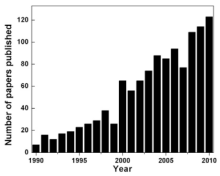

Fig. 1.
Number of papers published per year in the field of “bioactive glass” (compiled from a literature search in Web of Science carried out in December 2010).

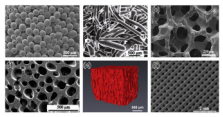

Fig. 2.

Microstructures of bioactive glass scaffolds created by a variety of processing methods: (a) thermal bonding (sintering) of particles (microspheres); (b) thermal bonding of short fibers; (c) “trabecular” microstructure prepared by a polymer foam replication technique; (d) oriented microstructure prepared by unidirectional freezing of suspensions (plane perpendicular to the orientation direction); (e) X-ray microCT image of the oriented scaffold shown in (d); (f) grid-like microstructure prepared by robocasting. Glass composition: (a) $16CaO{-}21Li_2O{-}63B_2O_3$; (b–e) 13–93; (f) 6P53B.

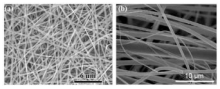

Fig. 3.
SEM images of nanofibrous bioactive glass: (a) borosilicate 13–93B1 glass with diameters in the range 150–450 nm prepared by electrospinning of a precursor solution (courtesy of C. Gao; Shinshu University, Japan); (b) bioactive glass with diameters in the range 100–800 nm, prepared from a melt-derived glass (courtesy of Mo-Sci Corp., Rolla, MO, USA).

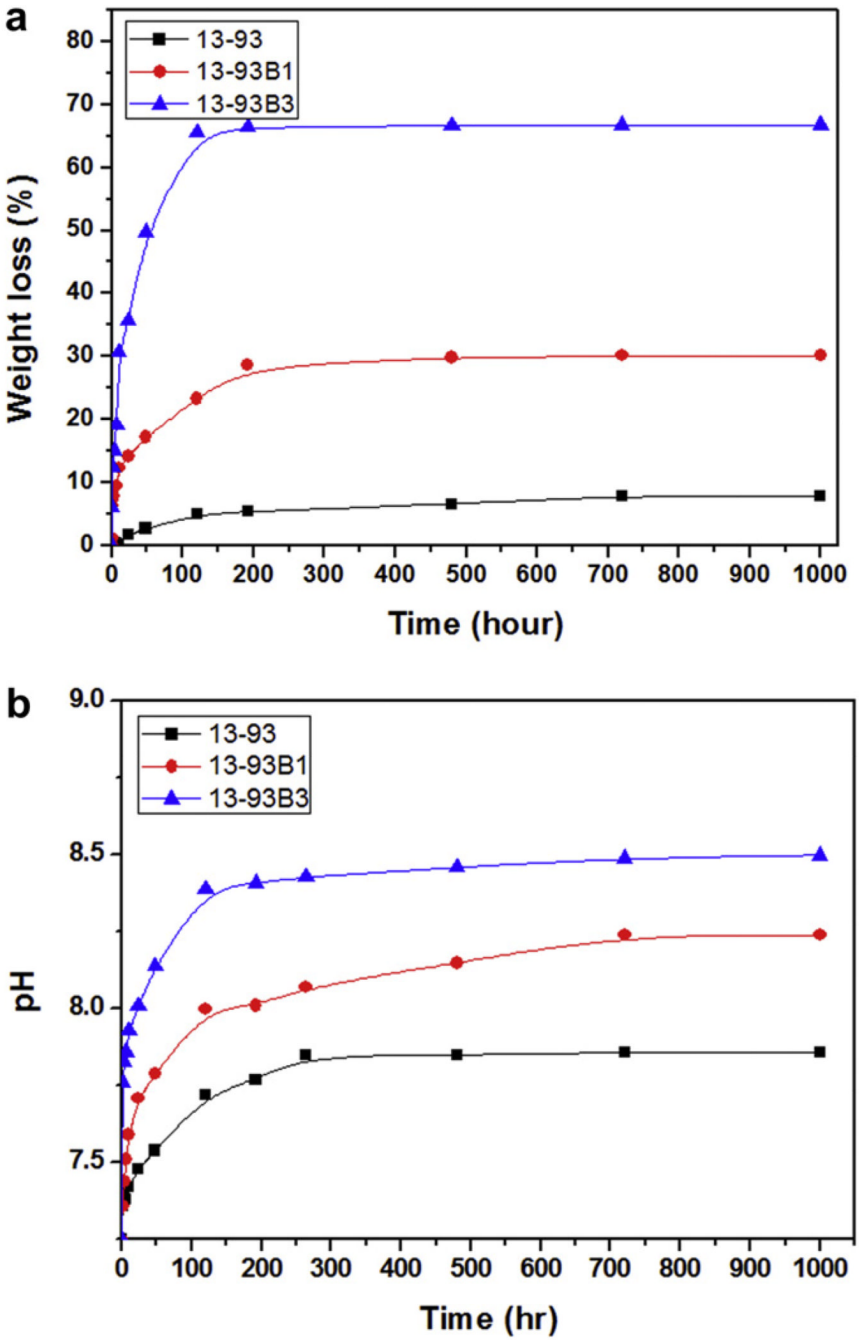

Fig. 4.

Degradation of bioactive glass scaffolds with a "trabecular" microstructure but with different compositions: silicate 13–93; borosilicate 13–93B1; borate 13–93B3, in SBF. The weight loss of the scaffolds (a), which provides a measure of the degradation of the scaffolds and their conversion to a hydroxyapatite-like material, and the pH of the solution (SBF) (b) are shown as a function of time. From Ref. [66].

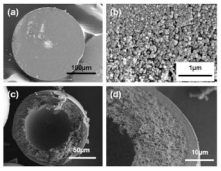

Fig. 5.

SEM images (low and high magnification) of the cross-section of porous or hollow HA particles prepared by converting bioactive borate glass particles with different CaO concentration in an aqueous phosphate solution at 37 °C: (a and b) porous HA microsphere formed by converting $41.5CaO{-}14.6Li_2O{-}43.9B_2O_3$ glass microspheres for 6 days in 1.5 M K_2HPO_4 solution at 37 °C and pH 9.0; (c and d) hollow HA microsphere formed by converting $16CaO{-}21Li_2O{-}63B_2O_3$ glass microspheres for 2 days in 0.02 M K_2HPO_4 solution at 37 °C and pH 9.0.

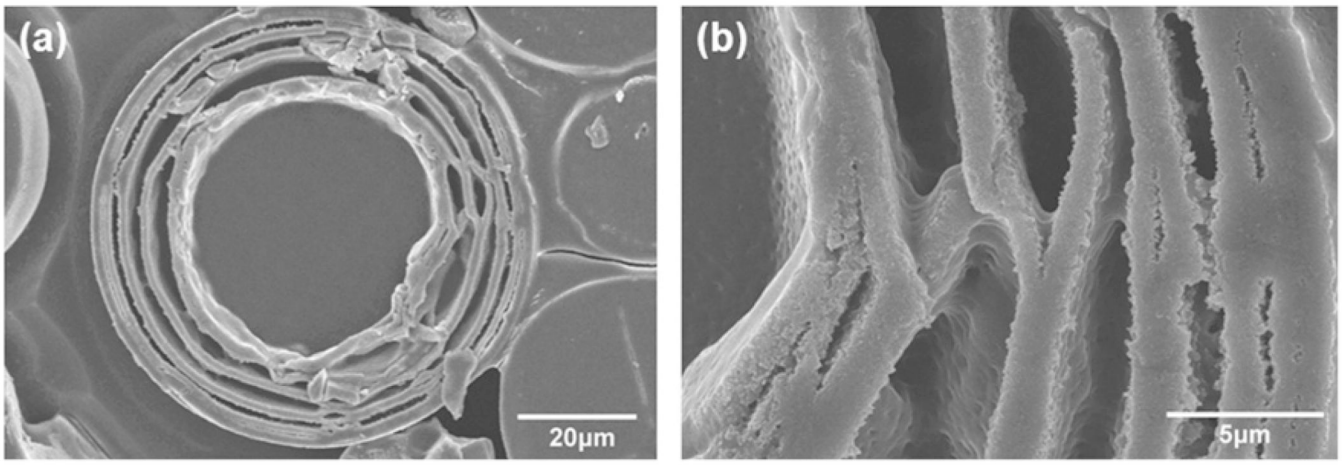

Fig. 6.
Lower and higher magnification SEM images showing the layered structure of HA microspheres formed by converting a bioactive glass with the composition $2Na_2O-2CaO-6B_2O_3$ in an aqueous phosphate solution at 37 °C.

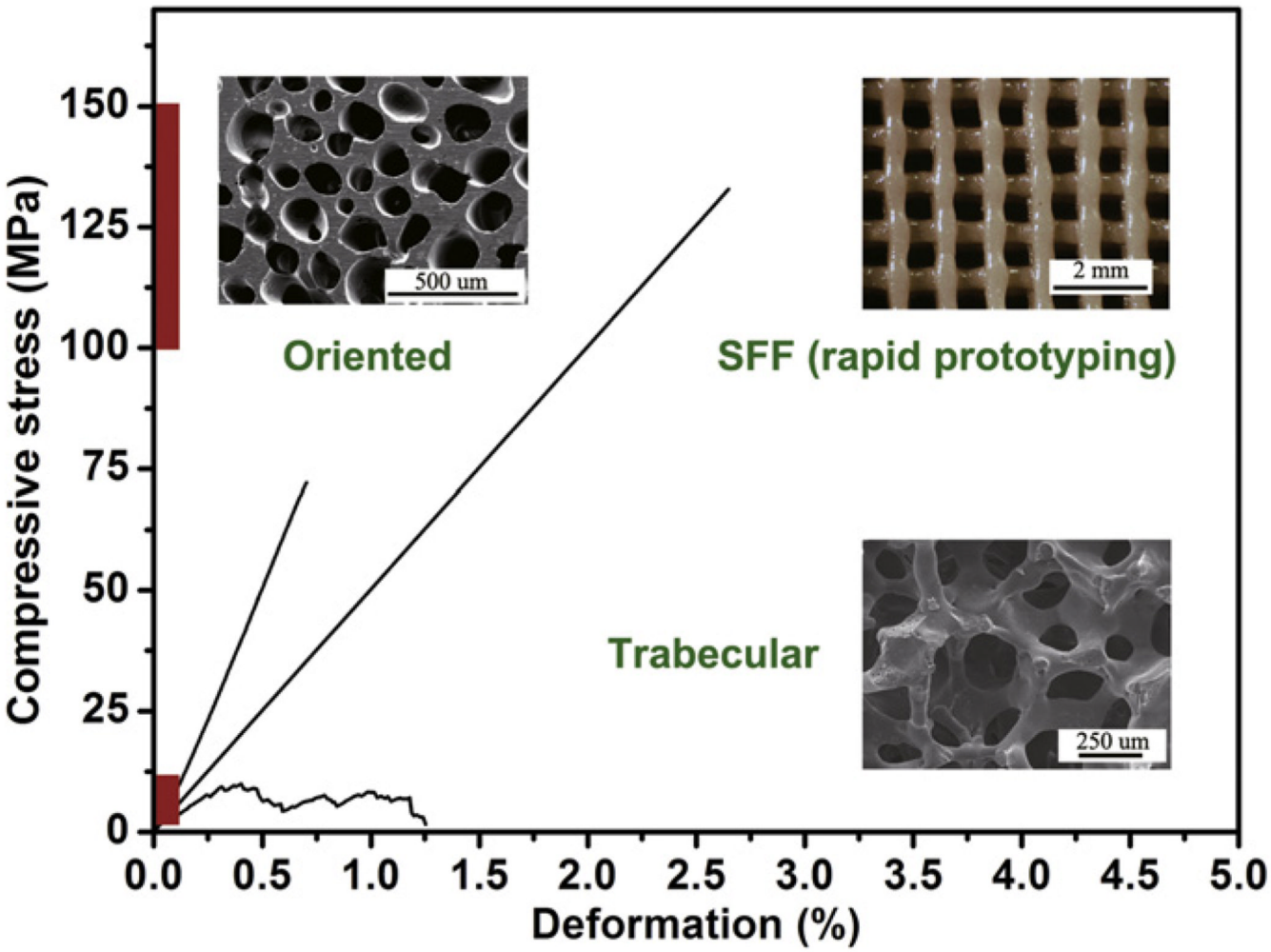

Fig. 7.

Mechanical response (compressive stress vs. deformation) of bioactive glass (13–93) scaffolds with: a trabecular microstructure prepared by a polymer foam replication technique; an oriented microstructure prepared by unidirectional freezing of suspensions; a grid-like microstructure prepared by freeze extrusion fabrication (a solid freeform fabrication technique). The ranges of compressive strength values for trabecular and cortical bone are shown in red.

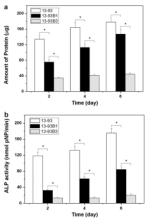

Fig. 8.
Ability of silicate 13–93, borosilicate 13–93B1 and borate 13–93B3 bioactive glass scaffolds with a trabecular microstructure to support (a) proliferation and (b) differentiated function of osteogenic MLO-A5 cells. Mean ± SD, $n = 4$. *Significant difference for glass scaffolds with different compositions ($p < 0.01$). From Ref. [77].

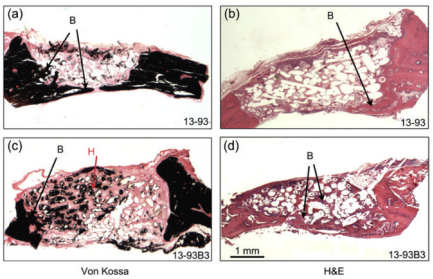

Fig. 9.

(Left) Von Kossa- and (right) H&E-stained sections of silicate 13–93 bioactive glass scaffolds (a and b) and borate 13–93B3 bioactive glass scaffolds (c and d), after implantation for 12 weeks in rat calvaria defects. B, bone; H, hydroxyapatite within scaffold. From Ref. [95].

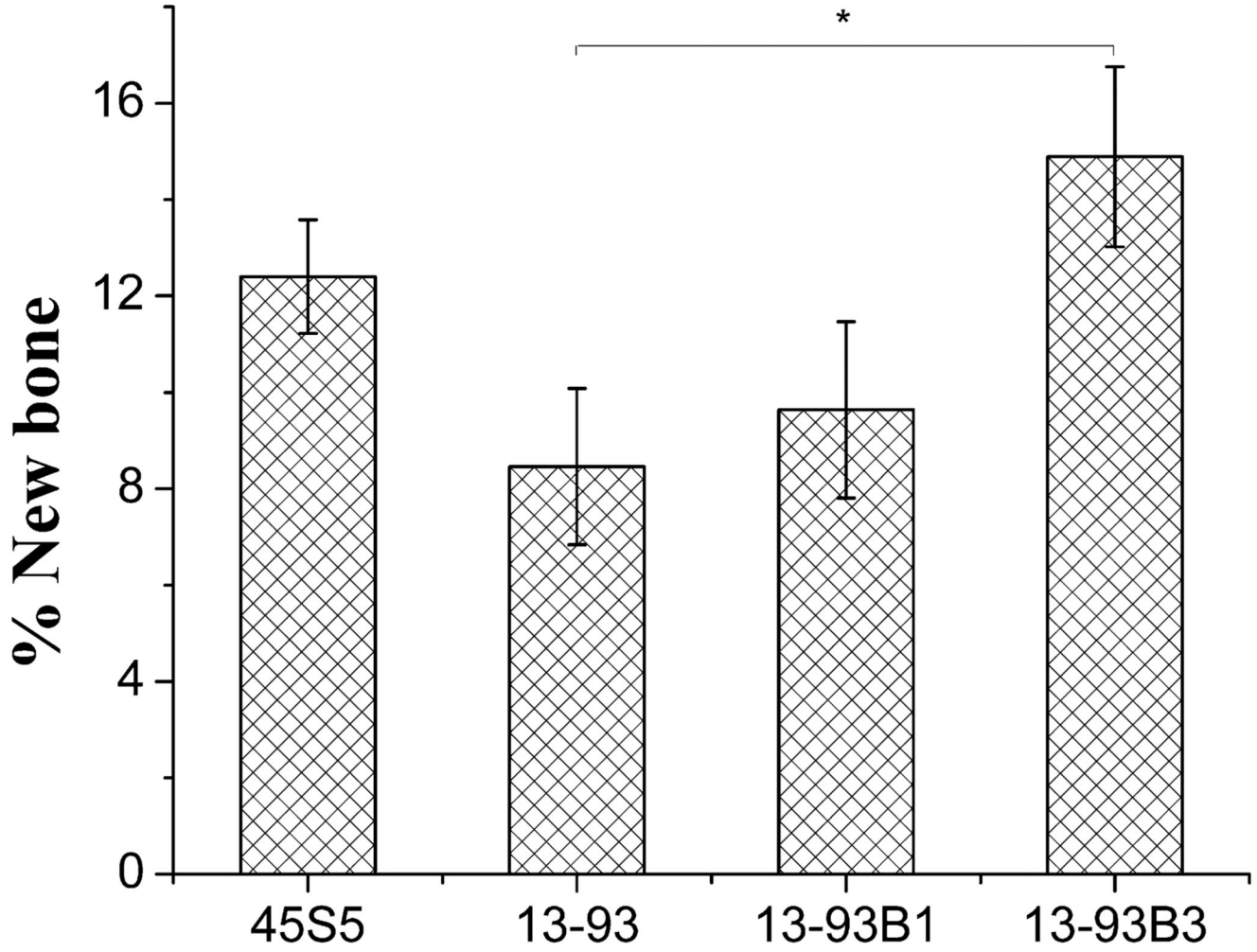

Fig. 10.
Percent new bone regeneration in rat calvarial defects implanted with “fibrous” scaffolds of silicate 13–93, borosilicate 13–93B1 and borate 13–93B3 bioactive glass, and with particles (150–300 μm) of 45S5 glass (*$p < 0.05$). From Ref. [95].

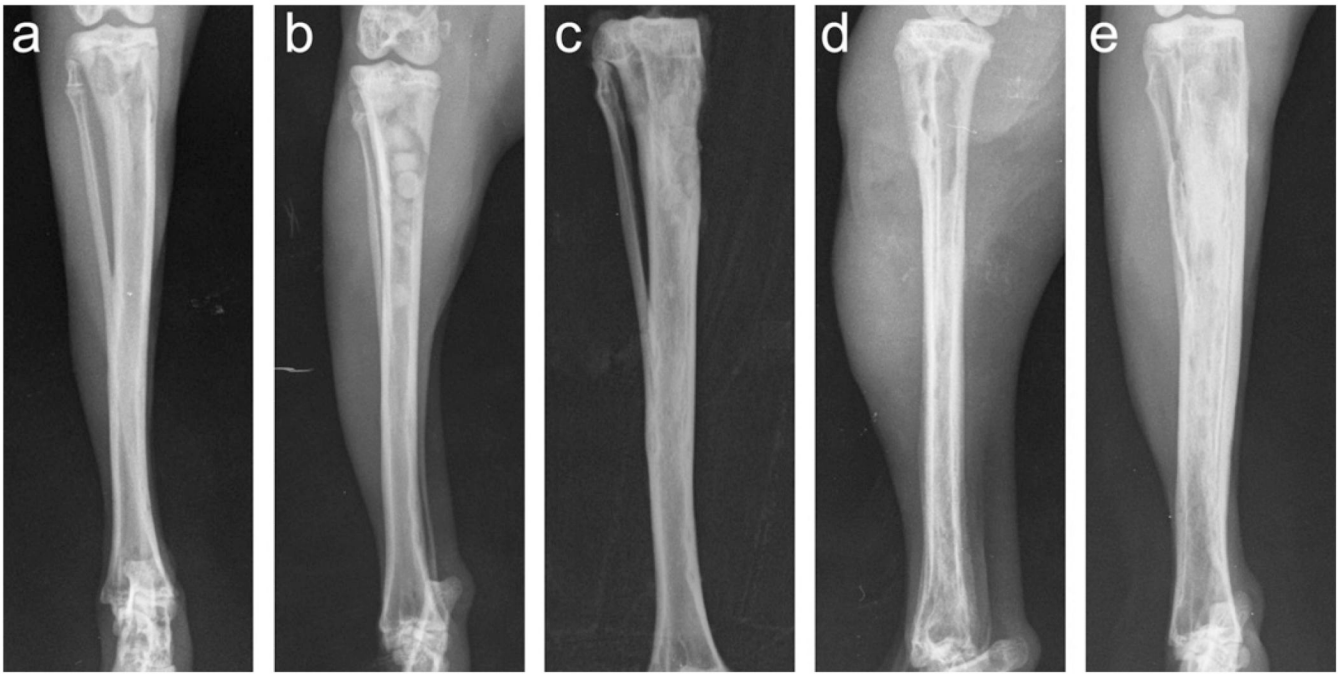

Fig. 11.

Radiographic images showing (a) experimental osteomyelitis in rabbit tibia induced by MRSA; (b) teicoplanin-loaded borate bioactive glass (TBDC) pellets implanted into rabbit tibia osteomyelitis model after debridement (group 1); (c) completely degraded TBDC pellets in rabbit tibia 12 weeks post-implantation; (d) the cleared cavity and bone window after debridement in group 2 animals (injected intravenously with teicoplanin); (e) evidence of deteriorated infection in group 2. From Ref. [80].

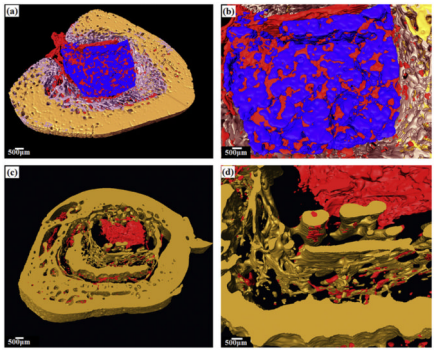

Fig. 12.

Synchrotron X-ray microCT shows three-dimensional reconstructed blocks of rabbit tibia osteomyelitis model 12 weeks post-implantation: (a and b) defect filled with teicoplanin-loaded borate bioactive glass, which converted to HA (blue) and formed new bone (light purple), while promoting angiogenesis (red); (c and d) empty defect. From Ref. [141].

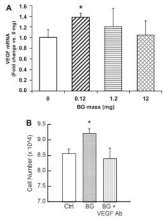

Fig. 13.

Bioactive glass (45S5; BG) induces the production of VEGF by human microvascular endothelial cells (HMVECs) cultured in indirect contact with the substrate. (A) Quantification of VEGF gene-specific mRNA by HMVECs exposed to varying amounts of BG. (B) HMVEC proliferation stimulated by BG–collagen sponges was inhibited by a soluble VEGF antibody (*$p < 0.05$ vs control). From Ref. [149].

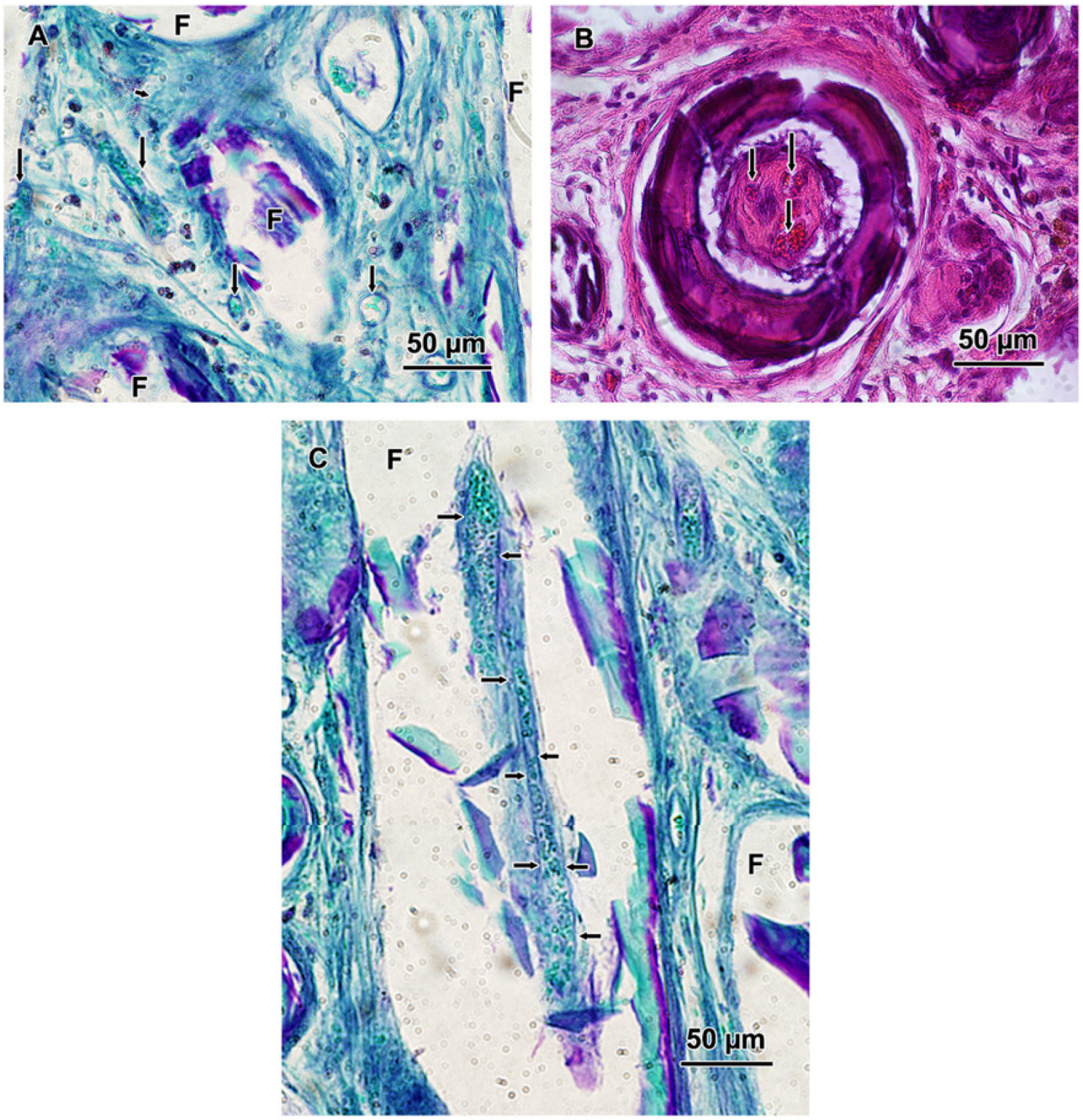

Fig. 14.

Light microscopy images of borate 13–93B3 bioactive glass scaffold implanted for 4 weeks in the dorsum of rats. (A) PAS-stained section, showing the material from the original glass fibers F, with blood vessels (arrow) with red blood cells (bright green) inside; (B) H&E-stained section showing a borate glass fiber that reacted with the body fluids, converted to HA, became hollow, and was filled with tissue and blood vessels (arrow); (C) PAS-stained section along the longitudinal axis of a fiber, showing a blood vessel inside the void of a hollow fiber (arrow). From Ref. [101].

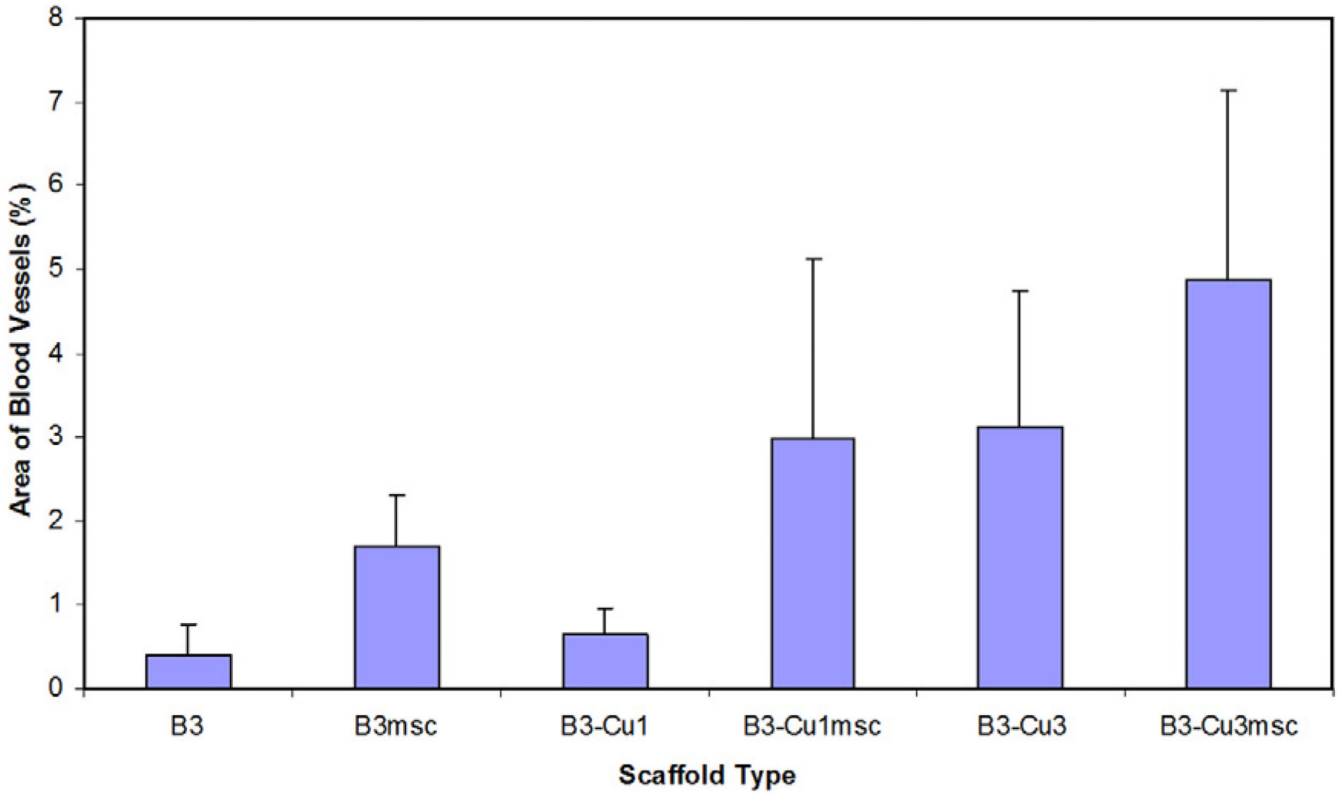

Fig. 15.

Effect of doping borate 13–93B3 bioactive glass scaffolds (B3) with copper (B3-Cu1: 0.1 wt.% Cu; B3-Cu3: 0.4 wt.% Cu) and/or seeding with bone marrow-derived MSCs (B3msc; B3-Cu1msc; B3-Cu3msc) on scaffold angiogenesis after six-week subcutaneous implantation in rats. From Ref. [101].

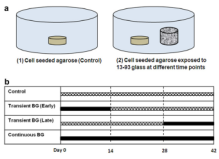

Fig. 16.

(a) Schematic of cell-seeded agarose incubated without or with a bioactive glass scaffold; (b) timeline for exposure of cell-seeded agarose to bioactive glass (black).

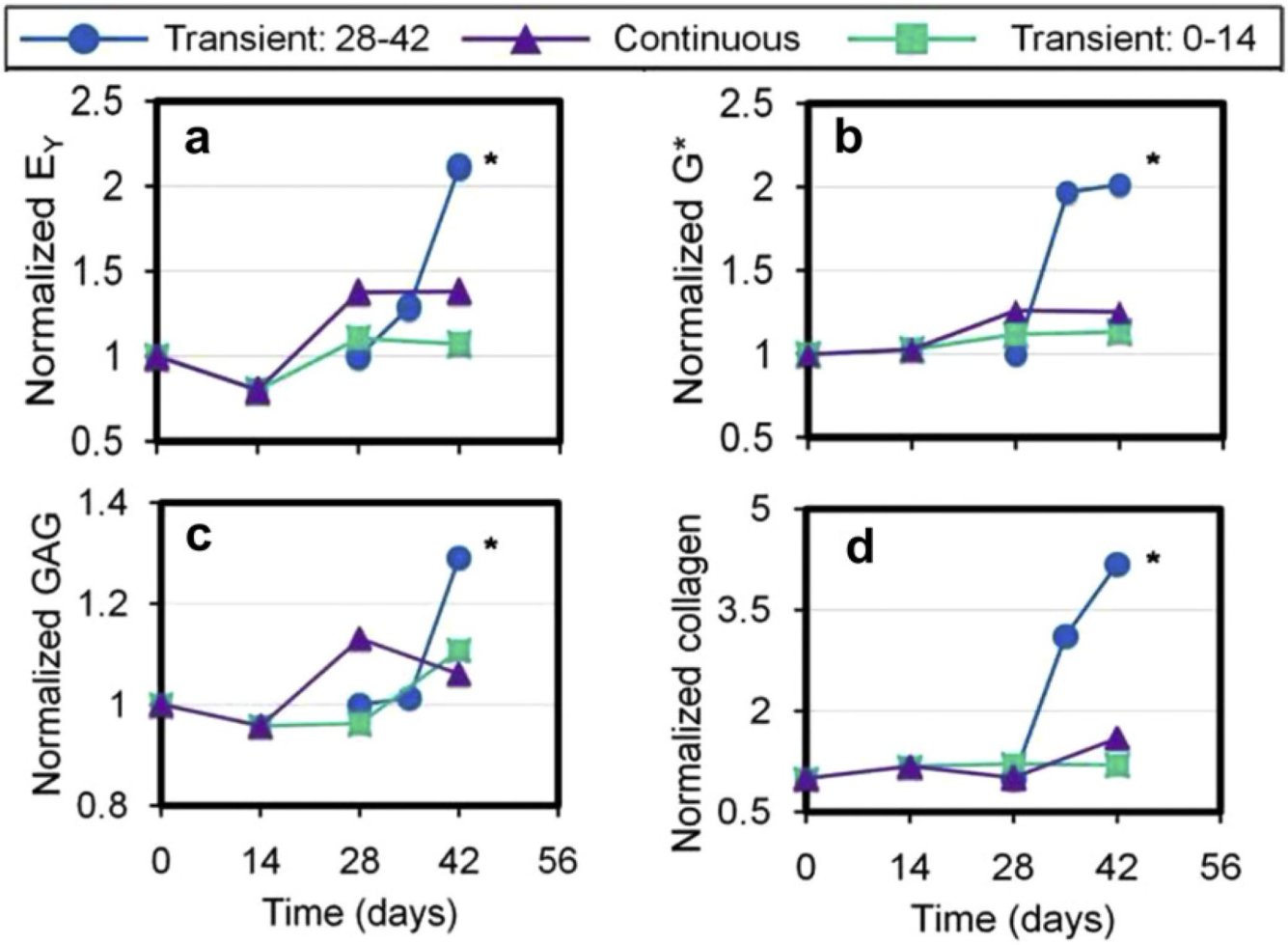

Fig. 17.

Mechanical and biochemical results as a function of time for chondrocyte-seeded agarose hydrogel co-cultured transiently or continuously with bioactive glass. The results are normalized to those for the agarose cultured without the bioactive glass. E_Y, equilibrium elastic modulus; G^*, dynamic elastic modulus; GAG, glycosaminglycan. From Ref. [156].

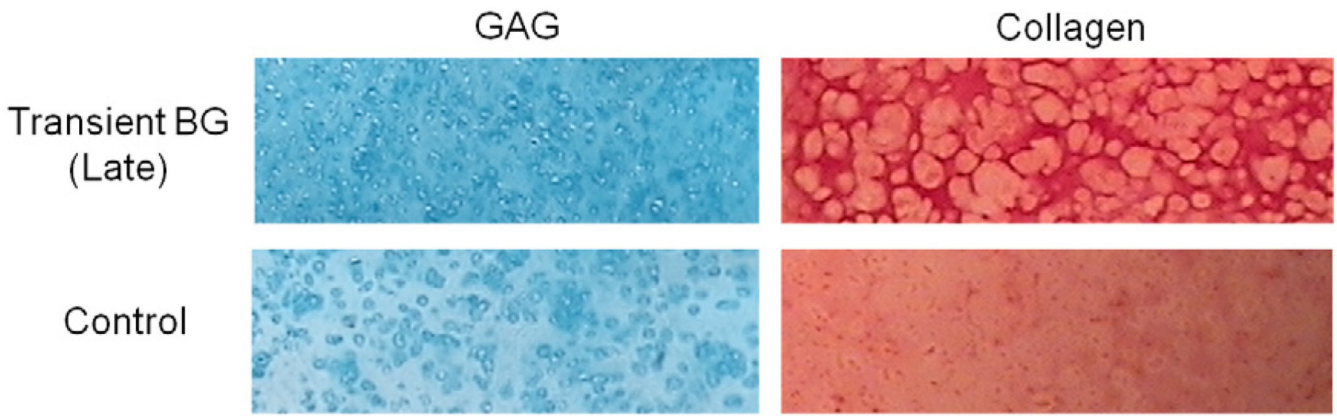

Fig. 18.

Alcian blue- (GAG) and picrosirius red-stained (collagen) histology images of cell seeded agarose cultured for 6 weeks; cell-seeded agarose cultured without bioactive glass (control) and cell-seeded agarose exposed to bioactive glass for the last 2 weeks of culture only (BG 13–93 construct) (magnification 10×). From Ref. [156].

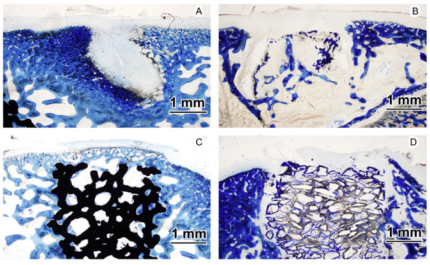

Fig. 19.

Histology at 12 weeks post-implantation with: (A) control (empty defect); (B) rabbit allograft; (C) trabecular tantalum; and (D) 13–93 bioactive glass. The best osteointegration scores were obtained with bioactive glass and tantalum. From Ref. [163].

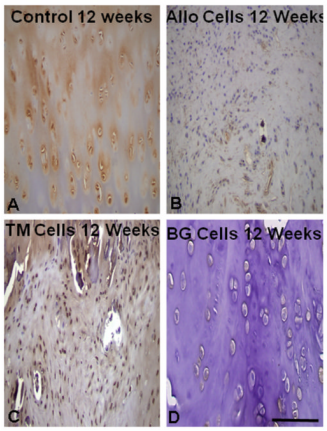

Fig. 20.

Collagen type II immunohistochemistry of the surface tissue at 12 weeks post-implantation for (A) control (no defect), and for cell-seeded agarose bonded to (B) rabbit allograft, (C) trabecular tantalum and (D) 13–93 bioactive glass. The surface tissue most closely resembled hyaline cartilage with trabecular tantalum and bioactive glass substrates. From Ref. [163].

Table 1

Compositions of various bioactive glasses.

Composition (wt.%)	45S5	13–93	6P53B	58S	70S30C	13–93B1	13–93B3	$P_{50}C_{35}N_{15}$
Na_2O	24.5	6.0	10.3	0	0	5.8	5.5	9.3
K_2O	0	12.0	2.8	0	0	11.7	11.1	0
MgO	0	5.0	10.2	0	0	4.9	4.6	0
CaO	24.5	20.0	18.0	32.6	28.6	19.5	18.5	19.7
SiO_2	45.0	53	52.7	58.2	71.4	34.4	0	0
P_2O_5	6.0	4.0	6.0	9.2	0	3.8	3.7	71.0
B_2O_3	0	0	0	0	0	19.9	56.6	0

Table 2

Methods used to create bioactive glass scaffolds, and characteristics of the fabricated scaffolds.

Method	Glass	Porosity (%)	Pore size (μm)	Strength* (MPa)	Reference
Thermal bonding of					
Particles	13–93	40–45	100–300	22 ± 1	[99]
Short fibers	13–93	45–50	>100	5	[127]
Polymer foam replication	45S5	89–92	510–720	0.4 ± 0.1	[63]
	13–93	75–85	100–500	11 ± 1	[102]
	13–93B3	80–85	100–500	5 ± 0.5	[66]
Sol–gel foam	70S30C	82	500 (100)*	2.4	[123]
Unidirectional freezing of suspensions	13–93	53–57	90–110	25 ± 3	[110]
	13–93	50–55	60–120	27 ± 8	[111]
	13–93	50	50–150	47 ± 5	[164]
Solid freeform fabrication					
Selective laser sintering	13–93	58–60	700–1000	15 ± 1	[120]
Freeze extrusion fabrication	13–93	50	300	140 ± 70	[119]
Robocasting	6P53B	60	500	136 ± 22	[118]

*Macropore diameter = 500 μm; interconnected pore diameter = 100 μm.